

DESIGN AND SIMULATION OF SOFT SWITCHING BOOST CONVERTER FOR PHOTOVOLTAIC SYSTEM

DEVENDRA KUMAR MISHRA



Department of Electrical Engineering

National Institute Technology, Rourkela-769008

DESIGN AND SIMULATION OF SOFT SWITCHING BOOST CONVERTER FOR PHOTOVOLTAIC SYSTEM

A THESIS SUBMITTED IN PARTIAL FULFILMENTS OF THE REQUIREMENTS FOR THE
AWARD OF THE DEGREE OF

Master of Technology
In
Industrial Electronics

By
DEVENDRA KUMAR MISHRA
Roll No: 213EE5346



Under the Guidance of
Dr. MONALISA PATTNAIK

Department of Electrical Engineering
National Institute Technology, Rourkela-769008

May 2015



NATIONAL INSTITUTE OF TECHNOLOGY

ROURKELA

CERTIFICATE

This is to certify that the project entitled “**DESIGN AND SIMULATION OF SOFT SWITCHING BOOST CONVERTER FOR PHOTOVOLTAIC SYSTEM**” submitted by Devendra Kumar Mishra (213ee5346) in partial fulfillment of the requirements for the award of Master of Technology degree in Industrial Electronics, Department of Electrical Engineering at National Institute of Technology, Rourkela is an authentic work carried out by her under my supervision and guidance.

To the best of my knowledge the matter embodied in this thesis has not been submitted to any other university/Institute for the award of any Degree.

Date:

Place: Rourkela

Dr. Monalisa Pattnaik

Department of Electrical Engineering

National Institute of Technology

Rourkela-769008

Email id: pattnaikm@nitrkl.ac.in

ACKNOWLEDGEMENT

On the submission of my thesis entitled “**DESIGN AND SIMULATION OF SOFT SWITCHING BOOST CONVERTER FOR PHOTOVOLTAIC SYSTEM**” I would like to extend my gratitude and sincere thanks to my supervisor **Dr. Monalisa Pattnaik**, Asst. professor, Dept. of Electrical Engineering for her constant motivation and support during the course work. I am very thankful to her for giving me good basics during the course work.

I would like to thank all others who have consistently encouraged and gave me moral support, without whose help it would be difficult to finish this project.

I would like to thank my parents and friends for their consistent support throughout.

Date:

Place: Rourkela

Devendra Kumar Mishra

Roll. No. 213EE5346

CONTENTS

ABSTRACT	i
LIST OF TABLES	ii
LIST OF FIGURES	iii
LIST OF ABBREVIATIONS	iv
LIST OF SYMBOLS	v
CHAPTER- 1 INTRODUCTION	1
1.1 Overview	1
1.1.1 Losses in Semiconductor Switches	1
1.1.2 Soft Switching	2
1.2 Literature Review	4
1.3 Motivation	5
1.4 Objective	6
1.5 Thesis Organization	6
CHAPTER-2 PHOTOVOLTAIC SYSTEM	6
2.1 Introduction	7
2.2 Arrangement of Proposed PV System	7
2.3 Mathematical Representation of PV	8
2.3.1 Single Diode Model	8
2.3.2 Double Diode Model	9
2.3.3 Large Array Simulation	10
2.4 Impact of Variation of Solar Irradiation	11
2.5 Effect of Variation of Temperature	11
2.6 PV Simulation	11
2.7 Simulation Results	12
2.8 Conclusion	14

CHAPTER- 3	MPPT CONTROL FOR PV SYSTEM	15
3.1	Introduction	15
3.2	Overview on MPPT	15
3.3	Incremental Conductance Algorithm	15
3.4	Flow Chart	17
3.5	Simulation Results	18
3.6	Conclusion	19
CHAPTER-4	SOFT SWITCHING BOOST CONVERTER	20
4.1	Introduction	20
4.2	Circuit Description	20
4.3	Circuit Operation	21
4.4	Theoretical Waveforms	26
4.5	Converter Design	27
4.5.1	Design of the Power Circuit	27
4.5.2	Design of the Auxiliary Circuit	29
4.6	Specifications for Converter Simulation	32
4.7	Steady State Analysis of Converter	33
4.8	Tabulation for Losses and Efficiency in Hard & Soft Switching	33
4.9	Tabulation of Current and Voltage Stresses	37
4.10	Simulation Results	39
4.11	Conclusion	39
CHAPTER-5	CONCLUSION	40
5.1	Conclusion	40
5.5	Scope for Future Work	40
REFERENCES		

ABSTRACT

India is among leading power producing countries but still we have an unreliable and inefficient electrical infrastructure. Photovoltaic power generation can be helpful to meet the requirements of electricity demand. In order to increase efficiency of PV system a soft-switching boost converter is adopted, which consists of an auxiliary resonant circuit having an auxiliary switch, two diodes with a resonant capacitor and a resonant inductor. This model of converter can supply 60 W to load. Since hard switching generates losses during turn on and turns off but in the proposed converter circuit Zero Voltage Switching operation is performed by resonant capacitor at turn-off condition and Zero Current Switching operation by resonant inductor at turn-on. The chosen converter reduces switching loss as well as voltage and current stress across the devices due to this the efficiency of converter increases. As designed converter is operated at high frequency, so small size of inductors and capacitors are required, this reduces size of converter. Incremental Conductance algorithm is used to achieve maximum power from PV module .The proposed converter and inverter circuit are simulated in Psim9.0 with PV and Maximum Power Point Tracking and theoretical analysis is verified.

LIST OF TABLES

Table. No.	Name of the table	Page. No.
2.1	Parameters of the simulated PV module	11
4.1	Component specifications of converter for simulation	27
4.2	Comparision of hard and soft-switching	38
4.3	Current and voltage stresses of various elements	39

LIST OF FIGURES

Fig. No.	Name of the Figure	Page. No.
1.1	Loss of Power during hard switching	2
1.2	(a) ZVS MOSFET implementation at turn off	3
	(b) Switching waveform of ZVS and hard switching	3
1.3	(a) ZCS MOSFET implementation at turn on	4
	(b) Switching waveform of ZCS and hard switching	4
2.1	Block diagram of proposed PV system	7
2.2	Photovoltaic cell single diode model	8
2.3	Photovoltaic cell two diode model	9
2.4	Photovoltaic array	10
2.5	Current-Voltage curve for PV module	12
2.6	Power-Voltage curve for PV module	12
2.8	Variation of I-V curve with solar irradiation	13
2.9	Variation of P-V curve with solar irradiation	13
2.10	Variation in I-V curve with Temperature	14
2.11	Variation in P-V curve with temperature	14
3.1	P-V curve locating MPPT	16
3.2	Flow chart of IC MPPT	17
3.3	Current curve at MPP	18
3.4	Voltage curve at MPP	18
3.5	Tracking of maximum power of PV	19
4.1	Circuit diagram of soft switching boost converter	20
4.2	Equivalent circuit of mode 1 for interval $[t_0-t_1]$	21
4.3	Equivalent circuit of mode 2 for interval $[t_1-t_2]$	22
4.4	Equivalent circuit of mode 3 for interval $[t_2-t_3]$	23
4.5	Equivalent circuit of mode 4 for interval $[t_3-t_4]$	24
4.6	Equivalent circuit of mode5 for interval $[t_4-t_5]$	25
4.7	Equivalent circuit of mode6 for interval $[t_5-t_6]$	26
4.8	Theoretical waveforms of converter	26

4.9	ZVS condition of switch	29
4.10	PWM signal for switch S_1, S_2	33
4.11	Main inductor current	34
4.12	Current and voltage across switch S_1, S_2	34
4.13	ZCS for switches S_1, S_2 at turn on	35
4.14	ZVS for switches S_1, S_2 at turn off	35
4.15	Resonant inductor current and resonant capacitor voltage	36
4.16	Output diode voltage and current	36
4.17	Output voltage of converter	38
4.18	Output power of converter	38

LIST OF ABBREVIATIONS

PV	Photo Voltaic
ZVT	Zero Voltage Transition
DC	Direct Current
MOSFET	Metal Oxide Semiconductor Field Effect transistor
PWM	Pulse Width Modulation
EMI	Electro-Magnetic Interference
ZVS	Zero Voltage Switching
ZCS	Zero Current Switching
MATLAB	MATrix LABoratory
PSIM	Powersim
MPPT	Maximum Power Point Tracking

P&O	Perturb and Observe
IC	Incremental Conductance

LIST OF SYMBOLS

T_{on}	Turn-on time of the switch
T_{off}	Turn-off time of the switch
P_{SW}	Switching Power losses
V_S	Voltage blocked by the switch
I_S	Flow of current allowed by the switch
f_s	Switching frequency of the converter
V_{in}	Input voltage
S_1	Main switch/boost switch
S_2	Auxiliary switch
L	Boost inductor
L_r	Auxiliary resonant inductor
C_r	Auxiliary resonant capacitor
D_1-D_2	Auxiliary circuit diodes
D	Boost diode
C_0	Output capacitor
t_0-t_6	Time instants in one switching cycle

I_{Lr}	Current flowing through the auxiliary circuit
V_{cr}	Voltage blocked by the resonant capacitor
P_{out}	Output power rating
V_{out}	Output voltage rating
V_{rp}	Output voltage ripple
ΔI_{rp}	Input peak current ripple
η	Efficiency of the converter
I_{min}	Input min current
I_{max}	Input max current
D	Duty cycle
ΔD	Duty Loss
f_r	resonant frequency
Z_r	Resonant impedance
I_{PV}	PV current
I_0	Diode's reverse saturation current
V_T	Diode's thermal voltage
K_I	Temperature coefficient of I_{sc}
K_V	Temperature coefficient of V_{oc}
G	Irradiance on the surface of the cell
G_{STC}	Irradiance under STC
I_{PV_STC}	Photocurrent generated under Standard Test Conditions (STC)

E_g	Energy gap of the semiconductor
I_{0_STC}	Nominal saturation current
I_{SC_STC}	Nominal value of I_{sc}
V_{OC_STC}	Nominal value of V_{oc}
N_{ss}	Number of modules in a serial connected string
N_{pp}	Number of strings that are connected in parallel
V_{mp}	Operating Voltage at MPP
I_{mp}	Operating Current at MPP
P_{max}	Maximum power
V_H	Unified voltage
$a_1 a_2$	Ideality constant of diode in two diode model
a	Ideality constant of diode in single diode model

CHAPTER-1

INTRODUCTION

1.1 Overview

This work is intended towards developing a soft-switching boost converter which is useful for Photovoltaic System. The main aim is to reduce switching losses by using a resonant circuit with conventional boost converter. Here MPPT algorithm is used for extraction of maximum power to ensure highly efficient operation of PV module. These converters consist of devices like diodes, BJTs, MOSFETs and IGBTs, which are used as switching devices. There should be wise selection of switching device depending upon power requirement and switching frequency. MOSFET is best suited for low power and low voltage applications whereas IGBT is used for higher power and higher voltage and current rating compared to MOSFET. IGBT's are operated in lower frequency range (up to 100 kHz) but MOSFET's are operated at much higher frequency range compared to IGBT. The proposed converter is operated under ZCS and ZVS condition which ensures improved efficiency, less electromagnetic interference etc.

1.1.1 Losses in Switching Devices

The devices used for switching in converters does not behave as ideal in experimental conditions, hence they are sources of loss of energy in the system. These losses are of two types which are described below:

Conduction losses:

The basic devices used normally are IGBT and MOSFET. The conduction losses in case of MOSFET are because of its nature of acting as resistor when it is fully turned on. The resistance is between drain to source resistance represented as R_{ds} . In case of IGBT the conduction loss depends on current passing through device during turn on condition and voltage $V_{ce,sat}$ offered across collector and emitter junctions.

Switching losses:

In practical conditions the voltage or current in the switch do not drop to zero when it is instantly turned on or off. So there is a time duration in which both current and voltage exists, so we can say there is overlapping area of voltage and current curve of switching device. Therefore this overlapping of curves causes power loss. Moreover as we know that average power is proportional to the frequency, so higher switching frequency will cause more loss. One more noticeable is the existence of EMI because of sharp and sudden transitions.

As it is clear from symbol of devices that both IGBT and MOSFET are having anti-parallel diodes but MOSFET has higher value of capacitance between drain and source as compared to capacitance between collector and emitter of IGBT. For MOSFET C_{ds} is charged with off stage voltage subjected to it and in case IGBT current tailing is observed even after turn off condition. AS we can observe that main losses for MOSFET are because of charging and discharging of the capacitance but for IGBT it is tailing current. The losses encountered in this situation are called hard switching losses. The losses are shown in Fig. 1.1.

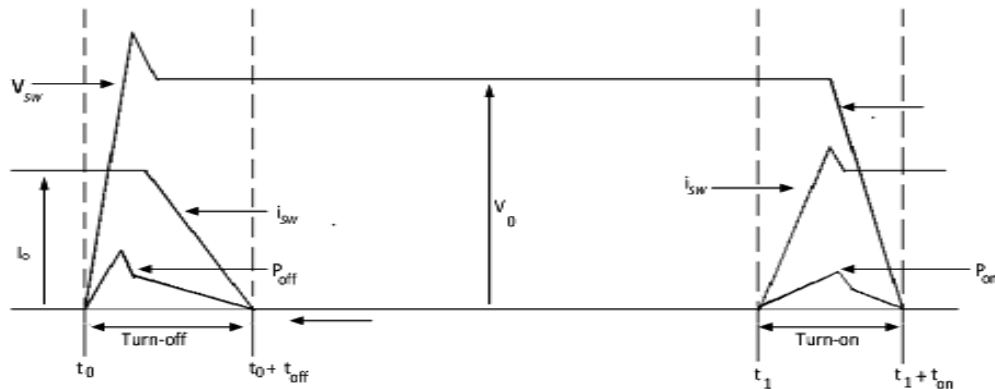


Fig. 1.1: Loss of Power during hard switching.

1.1.2 Soft Switching

The problems in case of hard switching like switching losses, EMI, current and voltage stresses can be reduced by using soft-switching method. The term "soft-switching" is subjected to gradual transitions of switch current and voltages. As transitions are gradual so di/dt and

dv/dt rating gets reduced so EMI reduction is observed and decrease in overlapping area between current and voltage curves is also seen because soft-switching makes any of the current or voltage to be zero when transition takes place. Therefore ideally there is no overlapping area between current and voltage curves of the switching device. These switching techniques are of two types: ZVS and ZCS. As in case of MOSFET it consists of capacitance C_{ds} which is actually combination of internal capacitance with additional external capacitance. MOSFET can be turned on with ZVS when it is sure that voltage across the switch just before the turned on is zero and MOSFET can turn off with ZVS because of C_{ds} which prevents abrupt rise in the voltage as the device is turned off [9]. Fig. 1.2 includes ZVS implementation using MOSFET and its switching waveforms.

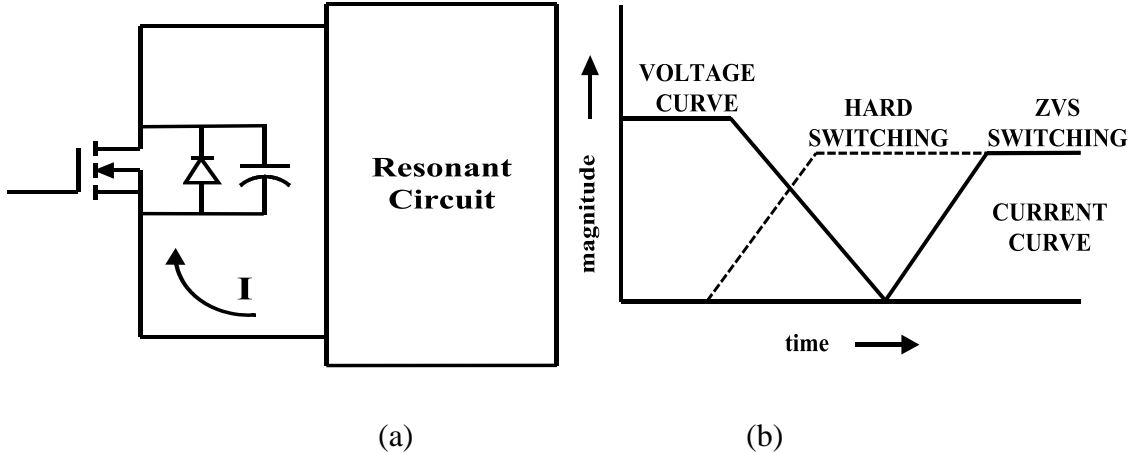


Fig. 1.2: (a) ZVS MOSFET implementation at turn off

(b) Switching waveform of ZVS and hard switching

ZCS operation can be performed by the switch if an inductor is connected in series with it. ZCS turn off can be achieved as inductor restricts rise in current which makes current through MOSFET nearly to zero. MOSFET turn off switch ZCS is achieved when negative voltage occurs across the combination (inductor-MOSFET) which causes gradual decay of current to zero because of inductor [11]. Fig. 1.3 includes ZCS implementation using MOSFET and its switching waveforms.

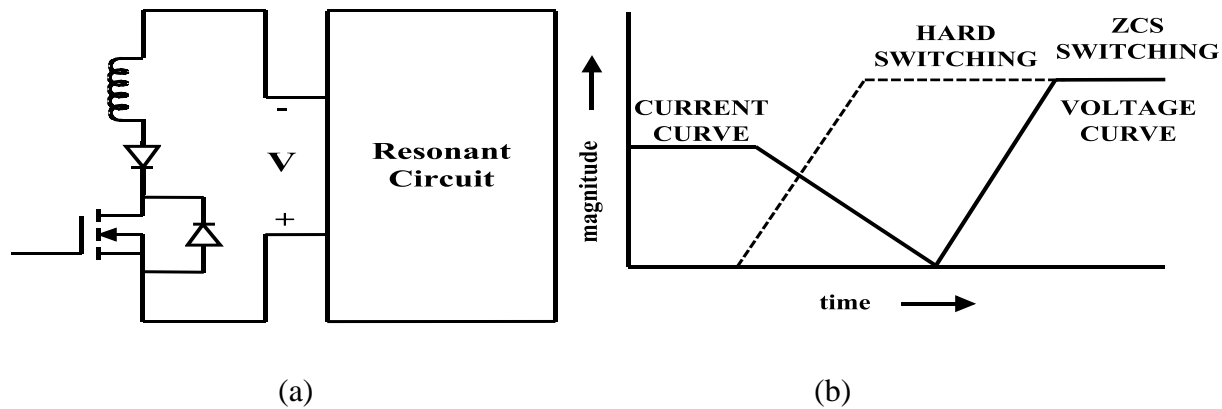


Fig. 1.3: (a) ZCS MOSFET implementation at turn on

(b) Switching waveform of ZCS and hard switching

Both MOSFET and IGBT can be used to perform ZVS and ZCS but for MOSFET, ZVS is preferred over ZCS and for IGBT ZCS is preferred over ZVS for IGBTs. When MOSFET is used for ZVS it can reduce the losses because of discharging of C_{ds} into device but in case of ZCS it cannot be done. As for the IGBT its capacitance lower so its main loss is turn off loss due to this tail in current is reduced with ZCS method.

1.2 Literature Review

In conventional hard switching converters, the conduction losses are very low. But high switching losses makes converters less efficient. So the technique of soft switching is introduced to make the switching transitions at either zero voltage condition or zero current condition, so that the dominating portion of losses (the ones caused due to switching under high voltages or currents) can also be reduced and the efficiency of the converters can be highly improved.

A soft switching converter is designed and its utility for PV system converter is verified in [1]. Detailed analysis on calculation of conduction and switching losses is done for soft switching boost converter and selection procedure of resonant element is discussed [2]. A review on various topologies of soft switching converters is discussed and compared their efficiency and other parameters. The discussion about isolated and non-isolated converters for PV system and their suitability according to requirement is done. This detailed analysis of various circuits of DC-DC boost converters on the basis of circuit complexity, efficiency is helpful for proper selection of method for converter design [3]. Three different topologies buck, boost and buck

boost are discussed with their steady state analysis and design of the auxiliary and main circuits are reported in [4]. A soft-switching inverter circuit is proposed which is operated with three phase induction motor, this useful for reducing the losses in the PV system after the operation of DC-DC converter [5]. A soft-switching converter using two switches main and auxiliary in which auxiliary switch is operated with some delay from the main switch, the losses due to switching for auxiliary switch reduces to zero. In this case higher voltage conversion ratio can be obtained whereas controlling is difficult in this case [6]-[9]. Design of digital PID controller for soft switching converters using pole placement technique is reported in [10]. Various ZCS circuits are reported and their comparative analysis is done in the literature [11]. An analysis of transformer less soft switching circuit with higher conversion ratio is proposed and their comparison with isolated converters is reported in [12]. A review on soft switching inverter circuits is presented in the paper [13]

Various papers have been referred soft switching methods for converter as well as for Photovoltaic cell and MPPT. The comprehensive model for PV cell is proposed, the single diode model and double diode is discussed, the equation related to this PV are derived, and the variation of current, voltage and power with change of irradiation and temperature is studied [14]-[16]. Incremental conductance MPPT is discussed and compared with other available MPPT methods, it observed that better response for Incremental conductance algorithm is observed as compared to Perturb and Observe algorithm. On the basis of complexity stability of MPP and other parameters selection of algorithms is justified [17]-[22].

1.3 Motivation

In our country demand of power is increasing day by day but the production is not increasing in that ratio. Electricity crises in summer season is very common but these are most hot days of the year and in this duration solar radiation availability is at peak, so solar power generation can be used more conveniently in this duration to fulfill the power requirement. The PV generation system uses converter circuit, while using conventional hard switching converter circuit efficiency of system reduces. This reduction in efficiency is due to switching loss, energy loss in stray L and C, device stress, thermal management, reverse recovery characteristics of diode. To overcome these losses, design soft switching converter circuit is the best among available solutions.

1.4 Objectives

The main objectives of this work are-

1. Reduction in power losses due to switching of MOSFETS by using soft switching cell.
2. Reduction in voltage stress and current stress of the switches and diodes.
3. Reduction in EMI problem caused by high $\frac{di}{dt}$ and $\frac{dv}{dt}$ rating by proper selection of resonant elements.
4. Simulation of proposed system and verification of theoretical analysis.

1.5 Thesis Organization

This thesis is manifested in chapter wise as follows:

Chapter 1

An overview of selection of soft switching technique over hard switching and renewable energy sources over other sources for power generation. Advantages soft switching over hard switching converters are listed. The motivation and objectives for this project are included.

Chapter 2

A brief discussion on proposed system, PV cell modeling with proper equivalent circuit and equations. PV characteristics and its variation with temperature and irradiation are explained with simulation results.

Chapter 3

An introduction to MPPT and its importance in solar PV power generation is presented. Mainly IC algorithm is presented in detail and simulation output of MPPT is discussed.

Chapter 4

A detailed analysis on soft switching boost converter and its need in solar power generation system is presented. The converter operation in six modes and corresponding equation are given. Simulation result of converter circuit with PV and MPPT is presented in this chapter.

Chapter 5

Conclusion of work done and futures aspect of the work is included.

CHAPTER 2

PHOTOVOLTAIC SYSTEM

2.1 Introduction

This chapter deals with the Photovoltaic system. A photovoltaic system is basically consist of few or large number of solar panels to get electrical energy from solar energy. It is composed of various component such as PV modules, mounting, mechanical and electrical connections and means of regulating output voltage of the system.

2.2 Arrangement of Proposed PV System

The PV system with MPPT is shown in the Fig. 2.1. The output voltage of PV is given to the converter, the current and voltage values are given to MPPT block which accordingly changes the duty cycle of pulses to extract maximum power. The obtained duty cycle given to PWM generator and it generates pulses, which are given to gate terminal of MOSFET switches.

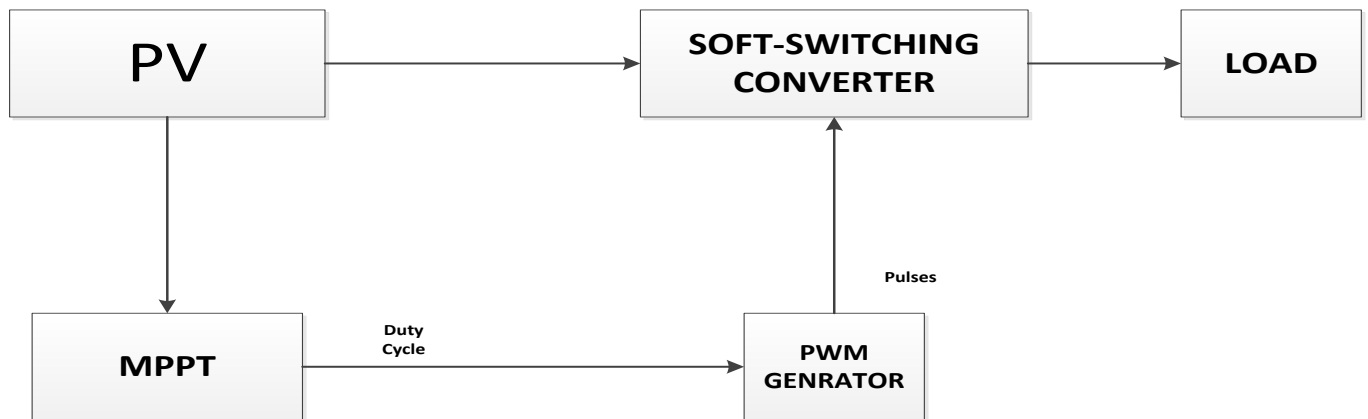


Fig. 2.1: Block diagram of proposed PV system

2.3 Mathematical Representation of PV

A PV cell can be represented mathematically by single and double diode models which are described below:

2.3.1 Single Diode Model

The single diode model [14] is shown below in Fig. 2.2 for a PV cell which includes a current source I_{PV} with a diode and a resistance in parallel and this structure is in series with resistance R_s .

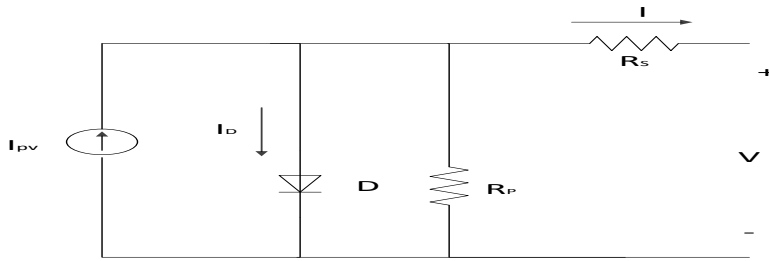


Fig. 2.2: Photovoltaic cell single diode model

The load current equation is given by

$$I = I_{PV} - I_0 \left[\exp\left(\frac{V + IR_s}{aV_T}\right) - 1 \right] - \left(\frac{V + IR_s}{R_p}\right) \dots \dots \dots (2.1)$$

In above equation I_{PV} represents photo current and I_0 is reverse saturation current which are given by equations (2.2) and (2.3).

$$I_{PV} = (I_{PV_STC} + K_I \Delta T) \frac{G}{G_{STC}} \dots \dots \dots (2.2)$$

$$I_0 = I_{0_STC} \left(\frac{T_{STC}}{T}\right)^3 \exp\left[\frac{qE_g}{ak} \left(\frac{1}{T_{STC}} - \frac{1}{T}\right)\right] \dots \dots \dots (2.3)$$

The equation (2.3) can be modified to (2.4) in terms of coefficients of current and voltages K_I and K_V as follows:

$$I_0 = \frac{(I_{SC_STC} + K_I \Delta T)}{\exp\left[\frac{(V_{OC_STC} + K_V \Delta T)}{aV_T}\right] - 1} \dots\dots\dots (2.4)$$

2.3.2 Double Diode Model

The single diode model neglects the recombination losses in depletion region. In actual practice these recombination losses causes a substantial loss, especially low voltages. This modeling is not possible using single diode model. To consider losses more precise two-diode model [15] is required, which is shown in Fig. 2.3.

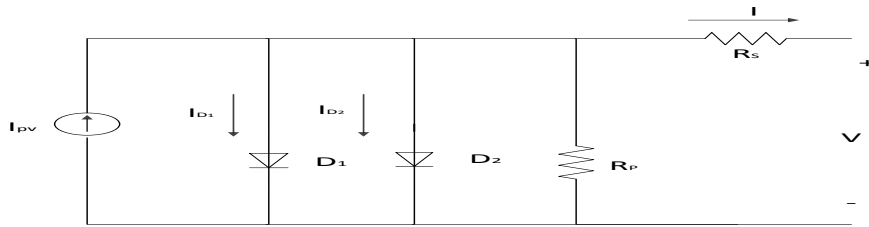


Fig. 2.3: Photovoltaic cell two diode model

The equations modelled for single diode model can be modified to get current expression for double diode model.

$$I = I_{PV} - I_{01} \left[\exp\left(\frac{V + IR_S}{a_1 V_T}\right) - 1 \right] - I_{02} \left[\exp\left(\frac{V + IR_S}{a_2 V_T}\right) - 1 \right] - \left(\frac{V + IR_S}{R_p}\right) \dots\dots\dots (2.5)$$

Where

$$I_{d1} = I_{01} \left[\exp\left(\frac{V + IR_S}{a_1 V_T}\right) - 1 \right] \dots\dots\dots (2.6)$$

$$I_{d2} = I_{02} \left[\exp\left(\frac{V + IR_S}{a_2 V_T}\right) - 1 \right] \dots\dots\dots (2.7)$$

$$I_{PV} = (I_{PV_STC} + K_I \Delta T) \frac{G}{G_{STC}} \dots\dots\dots (2.8)$$

$$I_{01} = I_{02} = \frac{(I_{SC_STC} + K_I \Delta T)}{\exp \left[\frac{(V_{OC_STC} + K_V \Delta T) / \left\{ \frac{a_1 + a_2}{p} \right\} V_T}{-1} \right]} \dots \dots \dots (2.9)$$

The diode ideal factors a_1 and a_2 represents recombination and diffusion components and on the basis of Shockley equation the value of a_1 is unity whereas value of a_2 is flexible. On the basis of simulations it can be found that a_2 is 1.2, so we can conclude $\left(\frac{a_1 + a_2}{p} = 1 \right)$. So equation (2.9) can be rewritten as

$$I_{01} = I_{02} = \frac{(I_{SC_STC} + K_I \Delta T)}{\exp \left[\frac{(V_{OC_STC} + K_V \Delta T) / V_T}{-1} \right]} \dots \dots \dots (2.10)$$

2.3.3 Large Array Simulation

For large power applications a series parallel structure (i.e. $N_{SS} \times N_{PP}$ modules), as shown in Fig.

2.4. The equation for PV can be modified as shown in equation (4.10) for single diode model [15].

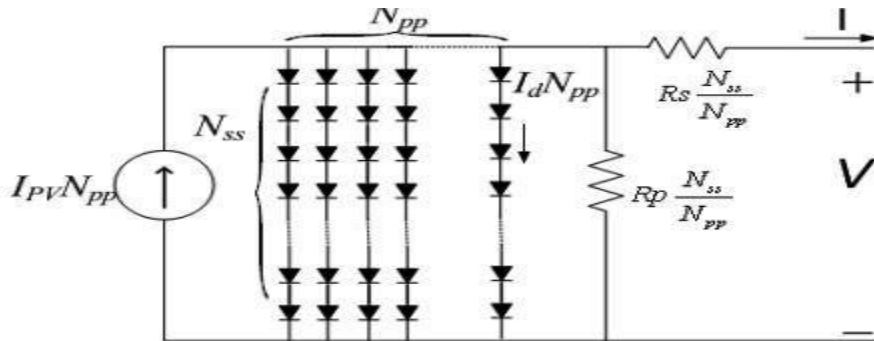


Fig. 2.4: Photovoltaic array

$$I = I_{PV} N_{PP} - I_0 N_{PP} \left[\exp \left(\frac{V + I R_S \left(\frac{N_{SS}}{N_{PP}} \right)}{a V_T N_{SS}} \right) - 1 \right] - \left(\frac{V + I R_S \left(\frac{N_{SS}}{N_{PP}} \right)}{R_P \left(\frac{N_{SS}}{N_{PP}} \right)} \right) \dots \dots \dots (2.11)$$

2.4 Impact of Varying Solar Irradiation

The characteristics of a PV cell are highly sensitive to solar irradiation. It keeps on fluctuating, due to the fact that environmental conditions changing continuously. Solar irradiation affects the PV input, the more is the irradiation, and consequently more will be the input to the PV cell. As result power value will be increased to the same voltage value. It also affects the open circuit voltage; it varies proportionally with the solar irradiation. The reason of this variation is movement of the electrons to higher energy level [16]. This movement increases mobility of electrons thereby increase in power also.

2.5 Effect of Variation of Temperature

Variation of temperature has a negative impact on PV cell i.e. it affects the power generation capacity. With an increase in temperature, open circuital voltage decreases. Because with the hike in temperature band gap energy of the semiconducting material increases [14]. Therefore required energy to jump the energy barrier increases and hence the efficiency reduces. The result section includes two figure showing how the P-V& I-V curve changing with the temperature.

2.6 PV ArraySimulation

The MSX-60 PV module simulation is done in MATLAB simulinkusing the single diode model equations. The parameters used for simulating the PV module are as shown in the Table 2.1

Table 2.1 Parameters of the simulated PV module

Sl.No.	PARAMETER	SYMBOL	VALUE
1	Current at maximum power	I_{mp}	3.5 A
2	Voltage at maximum power	V_{mp}	17.1V
3	Short circuit current	I_{sc}	3.8 A
4	Maximum power	P_{max}	60 W
5	Open circuit voltage	V_{oc}	21.1 V
6	Temperature coefficient of V	K_v	$-(80\pm 10)mV/^{\circ}C$
7	Temperature coefficient of I	K_i	$(0.0065\pm 0.015)\%/^{\circ}C$

2.7 Simulation Results

Fig. 2.5 shows I-V curve of PV module at standard temperature condition (25°C) and constant irradiation (1000 W/m^2).

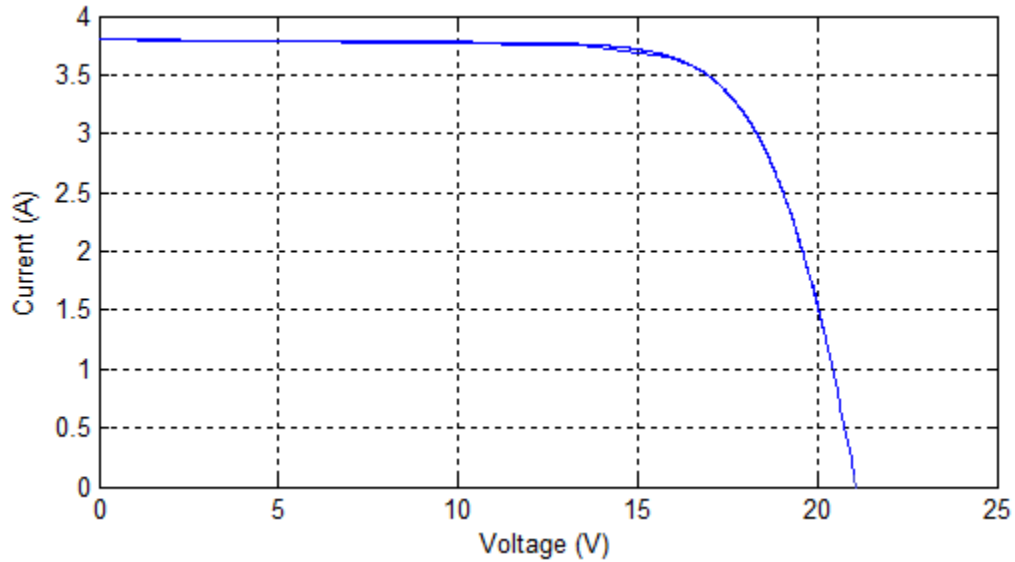


Fig. 2.5: Current-Voltage curve for PV module

Fig. 2.6 shows P-V curve of PV module at standard temperature condition (25°C) and constant irradiation (1000 W/m^2).

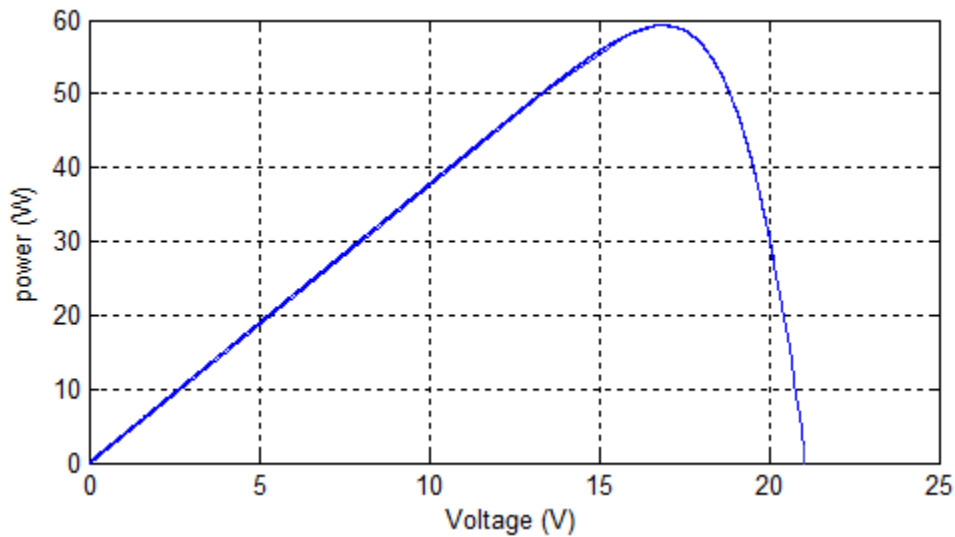


Fig. 2.6: Power-Voltage curve for PV module

Fig. 2.7 shows I-V curve of PV module at standard temperature condition (25 °C) and varying irradiation 1000 W/m², 800 W/m² and 600 W/m² respectively.

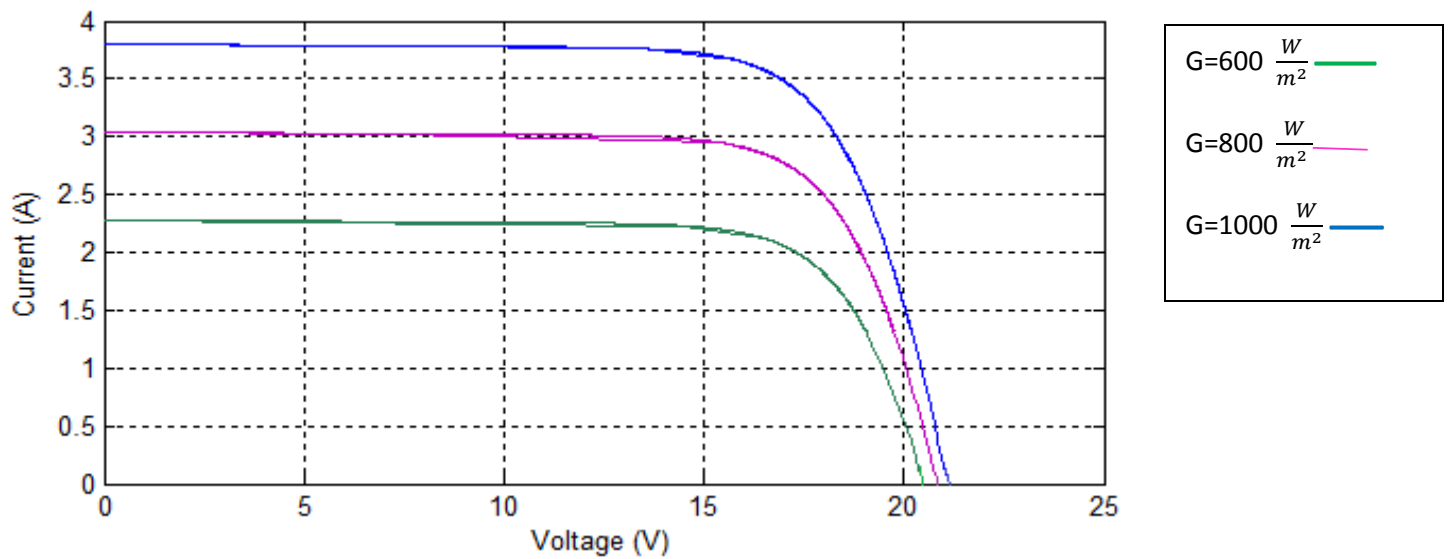


Fig. 2.7: Current-Voltage curve with variation of irradiation

Fig. 2.8 shows P-V curve of PV module at standard temperature condition (25 °C) and varying irradiation 1000 W/m², 800 W/m² and 600 W/m² respectively.

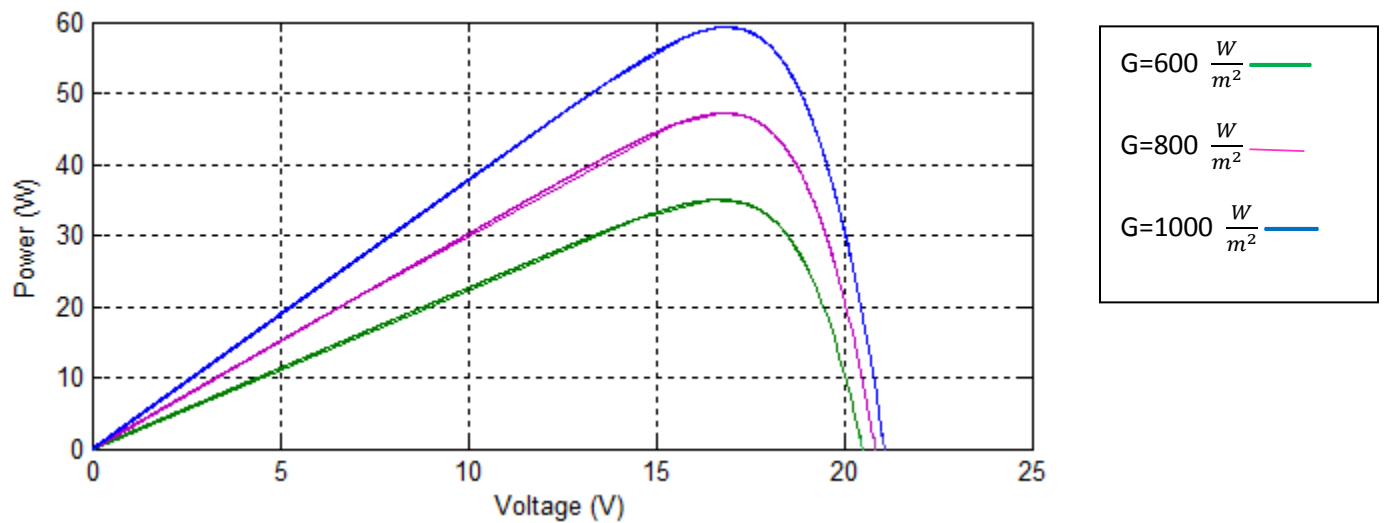


Fig. 2.8: Power-Voltage curve with variation of irradiation

Fig. 2.9 shows I-V curve of PV module at constant irradiation (1000 W/m²) and varying temperature 25 °C.

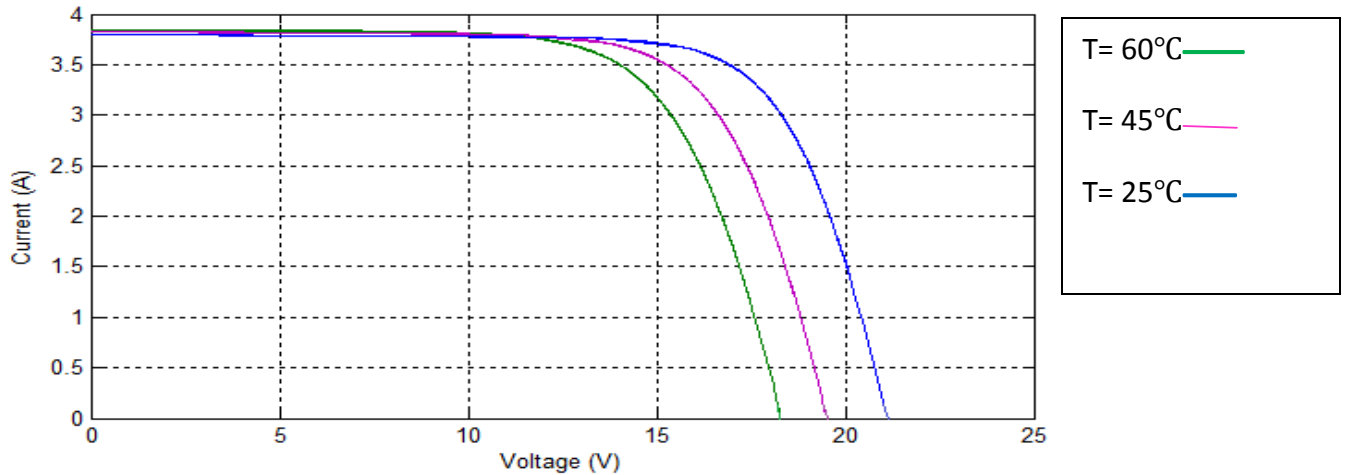


Fig. 2.9: Current-Voltage curve with variation of temperature

Fig. 2.10 shows P-V curve of PV module at constant irradiation (1000 W/m^2) and varying temperature

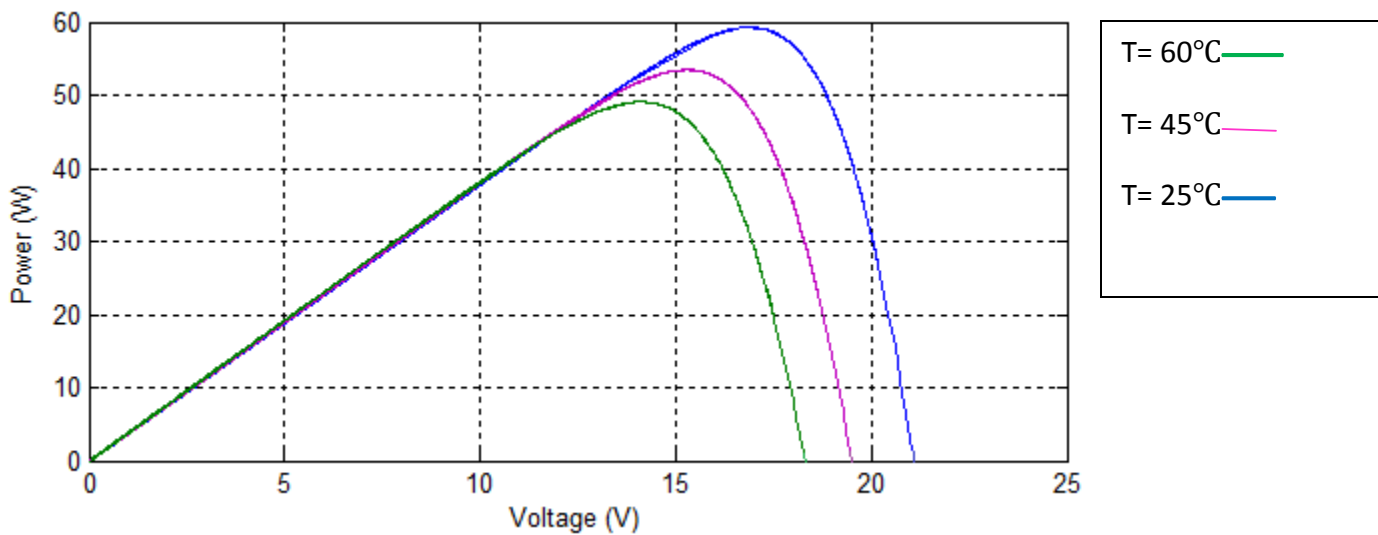


Fig. 2.10: Power-Voltage curve with variation of temperature

2.8 Conclusion

This chapter illustrates the basic idea on PV. Two different model of PV are discussed. PV model is properly described using equivalent circuit diagram along with all the relevant equation. The parameters taken during simulation listed in a table. The simulation results of P-V and I-V characteristics are included.

CHAPTER-3

MPPT CONTROL FOR PV SYSTEM

3.1. Introduction

This chapter mainly discuss about the Maximum power point tracking circuit. Types and process of tracking are described here. It gives mainly basic idea on Incremental conductance method with flow chart.

3.2 Overview on MPPT

PV system's efficiency depends on MPPT. MPPT is the most important in PV system. The efficiency of a PV system largely depends on MPPT and main cause of shifting of MPP (Maximum Power Point) is change in temperature and irradiation given to the PV [17]. Moreover it is clear that PV has nonlinear characteristics so it becomes more necessary to use MPPT.

There are various methods available for the tracing of MPPT some of them are named below:

1. Perturb and observe method
2. Incremental conductance algorithm
3. Fuzzy logic control method
4. Fractional open circuit voltage
5. Fractional short circuit current etc.

Here “Incremental conductance” is selected for proposed PV system as it gives more rapid response as compared to P&O method and less oscillation.

3.3 Incremental Conductance Algorithm

This algorithm is used to conclude the sign of $\frac{dP}{dV}$ ratio and continuous observes the dynamic conductance ($\Delta I / \Delta V$) and it is compared with the static conductance (I / V) when both becomes

equal then MPP is achieved [18]. A set of mathematical equation can be written for more ease of understanding as:

The power is given by $P = VI$ (3.1)

$$I = \frac{dP}{dV} = \frac{d(VI)}{dV} = I \frac{dV}{dV} + V \frac{dI}{dV} = I + I \frac{dI}{dV} \dots\dots\dots (3.2)$$

So equations can be expressed as

$$\frac{dI}{dV} = -\frac{I}{V} \text{ Or } \frac{dP}{dV} = 0 \text{ At MPP} \dots\dots\dots (3.3)$$

$$\frac{dI}{dV} > -\frac{I}{V} \text{ Or } \frac{dP}{dV} < 0 \text{ Left of MPP} \dots\dots\dots (3.4)$$

$$\frac{dI}{dV} < -\frac{I}{V} \text{ Or } \frac{dP}{dV} > 0 \text{ Right of MPP} \dots\dots\dots (3.5)$$

The above three equations from equation (3.3) to equation (3.5) describes the position of MPP with respect to slope of P-V or I-V curves. Fig. 3.1 is graphical representation of above equations.

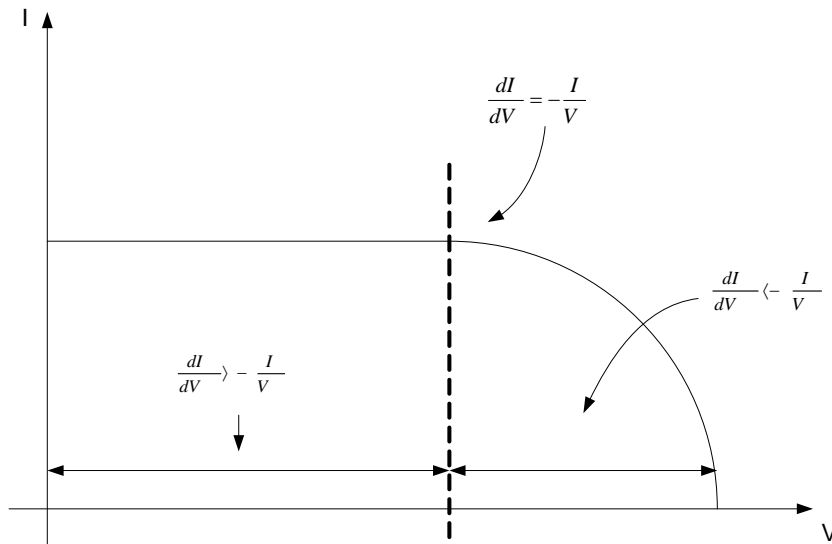


Fig. 3.1: I-V curve locating MPPT

3.4 Flow Chart

The flow chart for the MPPT algorithm using IC method is shown below in Fig. 3.2

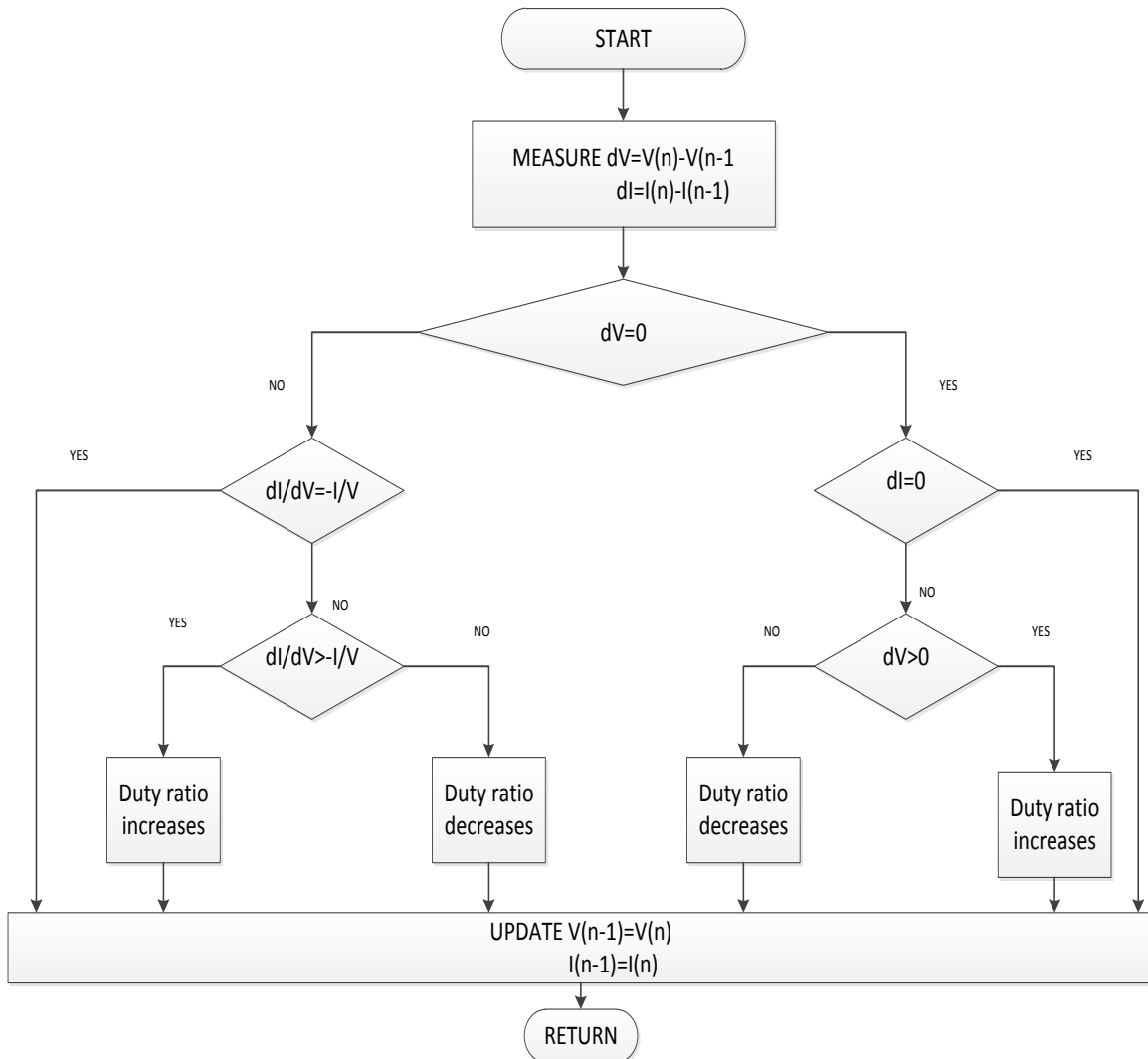


Fig. 3.2: Flow Chart of IC MPPT

3.5 Simulation Results

MPPT output of the PV system is shown below. Fig. 3.3 shows current of PV at maximum power point. Initially current fluctuates and later it goes steady. The obtained value of current at MPP is 3.68 A, which can be observed in Fig. 3.3.

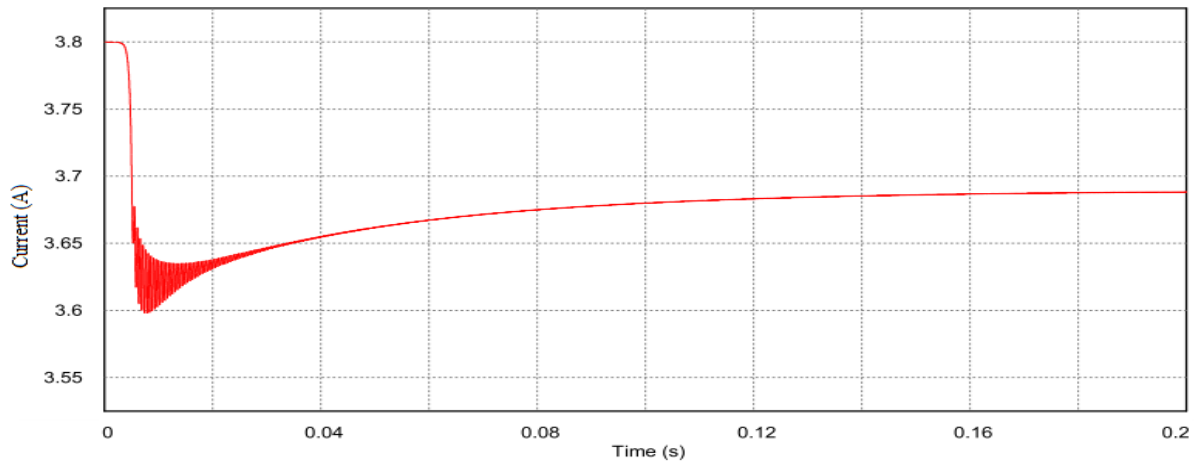


Fig. 3.3: Current curve at MPP

Fig. 3.4 shows voltage at MPP, initially voltage rises from zero and later goes steady. Here voltage at MPP is 17.1 V.

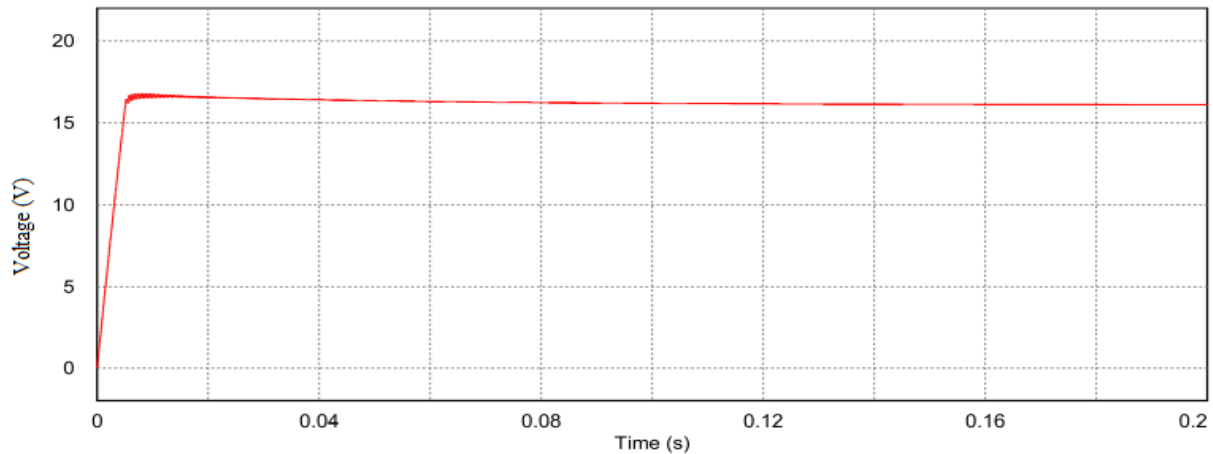


Fig. 3.4: Voltage curve at MPP

Fig. 3.5 shows power curve at MPP. Two labels for output tracked power curve of PV and maximum rated power curve of PV module. The obtained power at MPP is 59.5 W.

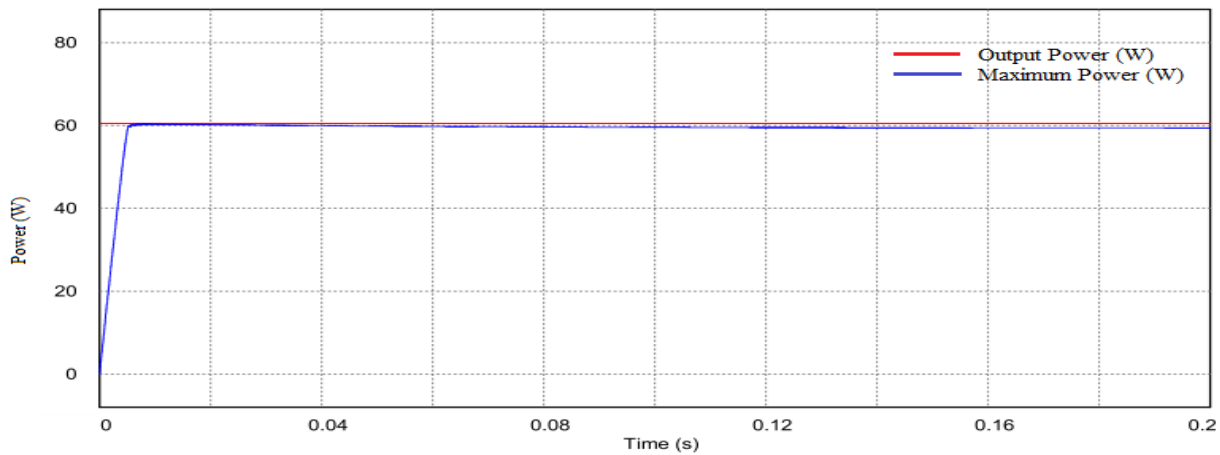


Fig. 3.5: Tracking of maximum power of PV

3.6 Conclusion

With the end of this chapter, it can be concluded that, MPPT is an important part for the PV system. As the curves obtained from PV system are nonlinear. Incremental conductance method is successfully demonstrated here with corresponding simulation results, relevant equation and flow diagram.

CHAPTER-4

SOFT SWITCHING BOOST CONVERTER

4.1 Introduction

This chapter gives an idea on soft switching boost converter. There are many DC-DC converters are available. For stepping up the voltage to some certain level, boost converter required. And the boost converter using soft switches make the whole system more efficient. How it increases the efficiency and details on soft switching technique are discussed.

4.2 Circuit Description

The circuit for soft switching converter is shown in Fig. 4.1 which consists of an extra soft-switching circuit which is not present in case of conventional boost converter. The auxiliary network comprises of an auxiliary switch (S_2) two diodes named as (D_1) and (D_2), resonant capacitor (C_r) and resonant inductor (L_r), whereas main circuit composed of main inductor (L_m), main switch(S_1), output capacitor (C_o) and Load (R). Supply is denoted as (V_{in}) which is actually voltage generated by PV and output voltage marked across load as indicated in Fig. 4.1

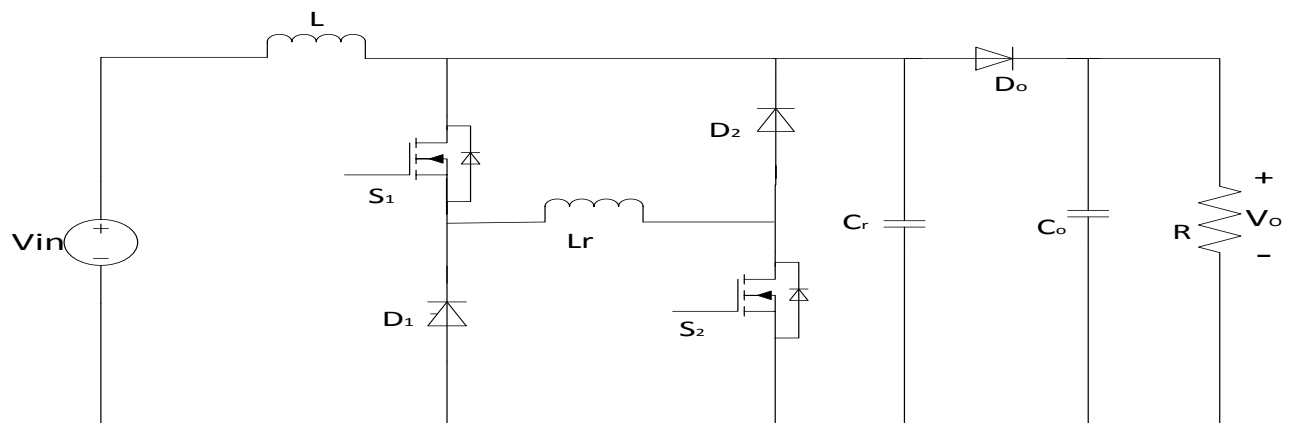


Fig. 4.1: Circuit diagram of soft switching boost converter

4.3 Circuit Operation of Soft-Switching Converter

The circuit for soft switching converter is operated in six modes [1]. The operation of the circuit in different modes is described below along with circuit diagrams and respective equations of those modes.

Mode 1 in the interval $[t_0-t_1]$

In mode 1 converter operates like conventional hard-switching converter and during this mode main and auxiliary switches S_1 and S_2 is in OFF condition. Current does not flows through resonant circuit but the load gets energy from the main inductor and main inductor current decreases linearly which is visible in waveforms shown in Fig. 4.2. Circuit and equations for this mode are shown below

$$V_L(t) = V_S - V_o \dots\dots\dots (4.1)$$

$$I_L(t) = I_L(t_0) - \left(\frac{V_o - V_S}{L} \right) t \dots\dots\dots (4.2)$$

$$I_{D_o}(t) = I_L(t) \dots\dots\dots (4.3)$$

$$I_{L_r}(t) = 0 \dots\dots\dots (4.4)$$

$$V_{C_r}(t) = V_o \dots\dots\dots (4.5)$$

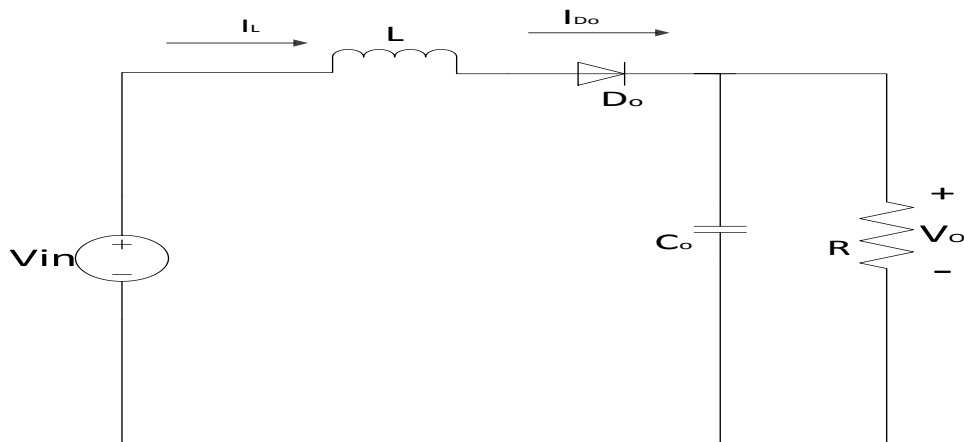


Fig. 4.2: Equivalent circuit of mode 1 for interval $[t_0-t_1]$

Mode 2 in the interval [t₁-t₂]

In this mode two switches S₁ and S₂ are turned on under ZCS due implementation of ZCS by main and auxiliary switches losses decreases. Here current through resonant inductor rises in this mode which results decrease in load current, when circuit operates at time t₂ current passing through diode D_o. Circuit diagram for this mode is shown in Fig. 4.3 and equation are shown below

$$I_{Lr}(t_1) = 0 \quad , \quad V_{Lr}(t) = V_o \dots\dots\dots (4.6)$$

$$I_{Lr}(t) = \left(\frac{V_o}{L_r}\right)t \dots\dots\dots (4.7)$$

$$I_L(t) = I_L(t_1) - \left(\frac{V_o - V_S}{L}\right)t \dots\dots\dots (4.8)$$

$$I_L(t_2) = I_{Lr}(t_2) \dots\dots\dots (4.9)$$

$$I_{D_o}(t_2) = 0 \dots\dots\dots (4.10)$$

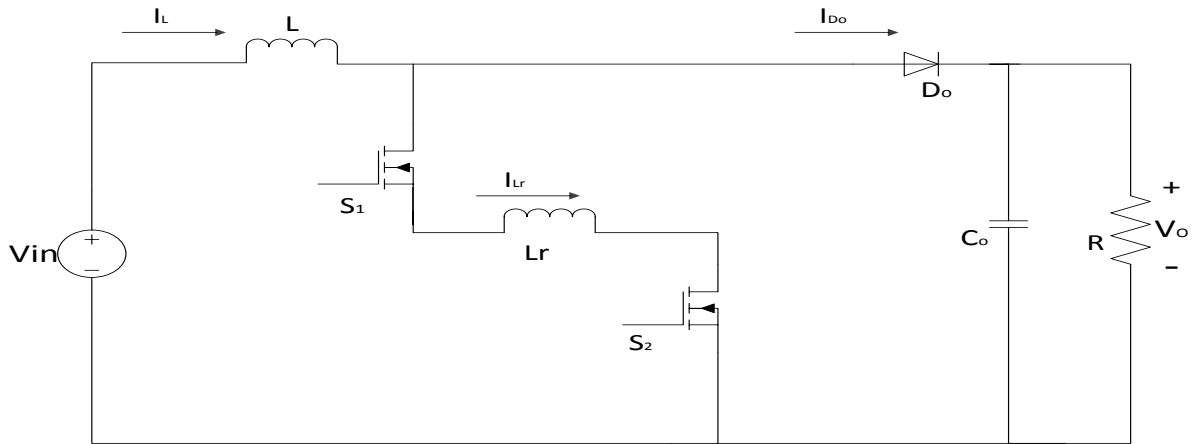


Fig. 4.3: Equivalent circuit of mode2 for interval [t₁-t₂]

Mode 3 in the interval [t₂-t₃]

The condition of resonance occurs in this mode and current through diode D_o becomes zero
 Expression for currents are as follows

$$I_L(t) = I_{\min} \dots \dots \dots (4.11)$$

$$I_{Lr}(t) = I_{\min} + \left(\frac{V_o}{Z_r} \right) \sin \omega t \dots \dots \dots (4.12)$$

The charging of C_r to voltage V_o and then discharging to zero. The required expression of impedance and resonant frequency are discussed in equations

$$V_{Cr}(t) = V_o \cos \omega_r t \dots \dots \dots (4.13)$$

$$V_{Cr}(t_2) = V_o \quad , \quad V_{Cr}(t_3) = 0 \dots \dots \dots (4.14)$$

$$Z_r = \sqrt{\frac{L_r}{C_r}} \quad , \quad \omega_r = \frac{1}{\sqrt{L_r C_r}} \dots \dots \dots (4.15)$$

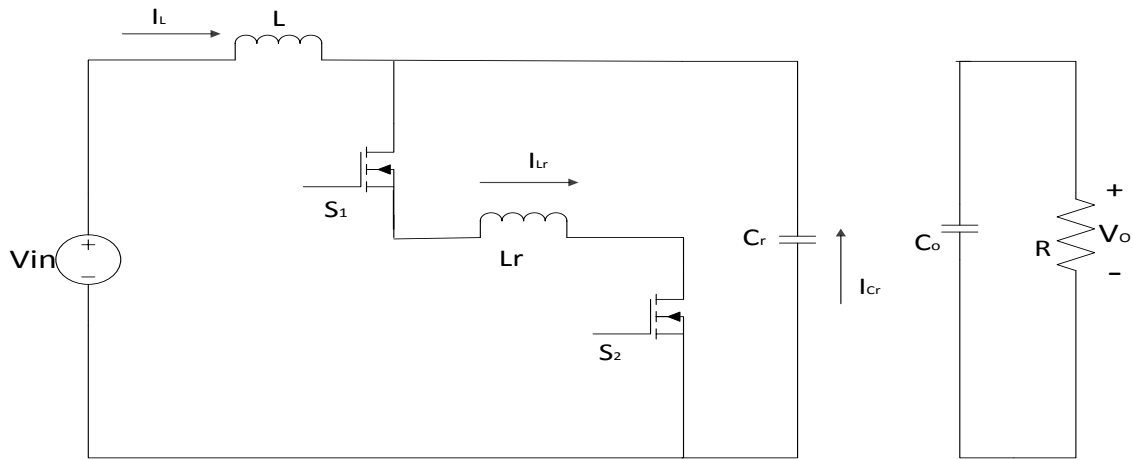


Fig. 4.4: Equivalent circuit of mode 3 for interval [t₂-t₃]

Mode 4 in the interval [t₃-t₄]

This mode operates in ZVS condition as current through resonant inductor is higher than main inductor both diodes of auxiliary circuits are in ON state. Path of current flow in circuit diagram shown in Fig. 4.5. Equations for resonant inductor and main inductor current and voltages are from equation (4.16) to equation (4.19).

$$I_{Lr}(t) = I_L(t) + I_{D1}(t) + I_{D2}(t) \dots\dots\dots(4.16)$$

$$I_{Lr}(t_3) = I_{Lr}(t_4) = I_{Lr,max} \dots\dots\dots(4.17)$$

$$V_L(t) = V_S \dots\dots\dots(4.18)$$

$$I_L(t) = I_{min} + \left(\frac{V_S}{L}\right)t \dots\dots\dots(4.19)$$

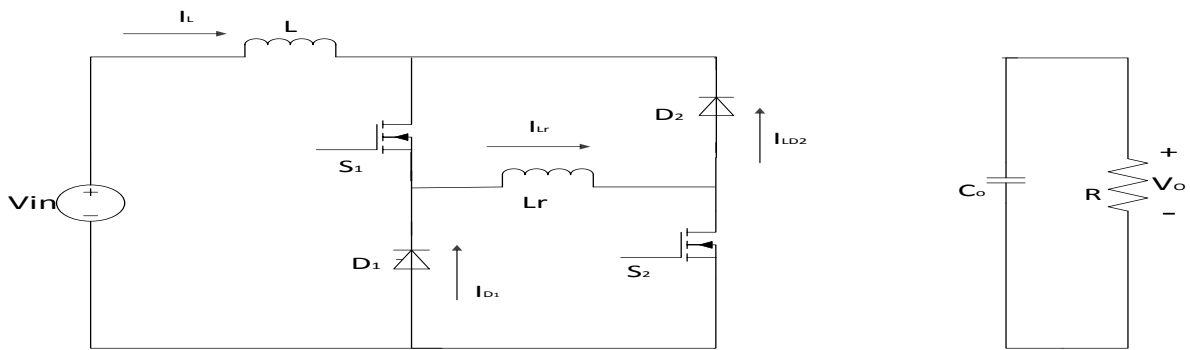


Fig. 4.5: Equivalent circuit of mode 4 for interval [t₃-t₄]

Mode 5 in the interval [t₄-t₅]

In this mode both switches are in OFF condition due to zero voltage condition of resonant capacitor. The voltages and currents for various elements in this mode are as follows:

$$I_{Lr}(t) = I_{max} - (I_{Lr,max} + I_{max}) \cos \omega t \dots\dots\dots(4.20)$$

$$I_{Lr}(t_4) = I_{Lr,max} \dots\dots\dots(4.21)$$

$$V_{Cr}(t_4) = 0 \dots\dots\dots(4.22)$$

$$I_L(t) = I_{\max} \dots\dots\dots (4.23)$$

$$I_{Lr}(t) = I_{\max} - (I_{Lr,\max} + I_{\max}) \cos \omega t \dots\dots\dots (4.24)$$

$$V_{Cr}(t) = Z_r (I_{Lr,\max} + I_{\max}) \sin \omega t \dots\dots\dots (4.25)$$

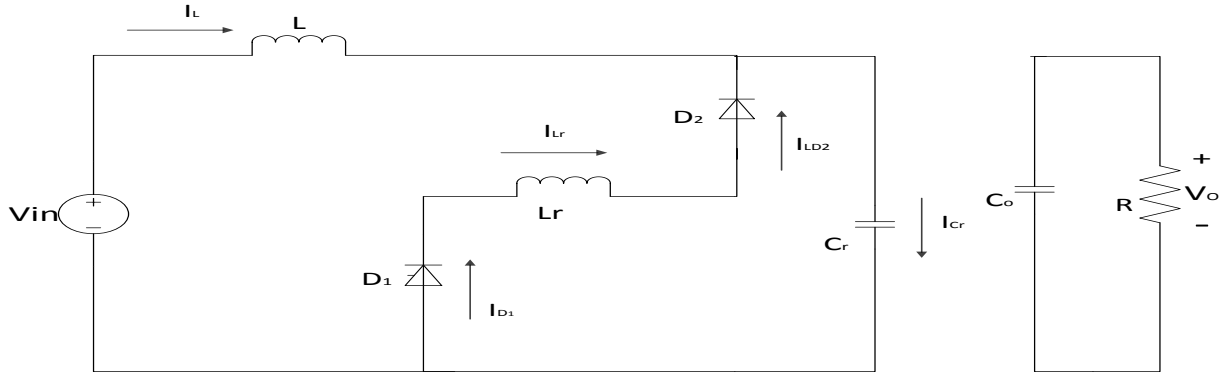


Fig. 4.6: Equivalent circuit of mode5 for interval [t₄-t₅]

Mode 6 in the interval [t₅-t₆]

It can be observed clearly that in the start of this mode the voltage across resonant capacitor reaches equal to output voltage, in another consequence output diode is turned on due to zero voltage condition.

$$I_{D_o}(t) = I_L(t) + I_{Lr}(t) \dots\dots\dots (4.26)$$

$$I_L(t_5) = (I_{Lr,\max} + I_{\max}) \cos \omega_r(t_5 - t_4) - I_{\max} \dots\dots\dots (4.27)$$

$$V_{Cr}(t) = V_o \dots\dots\dots (4.28)$$

Further decrease in main inductor and resonant inductor currents is observed and transfer of complete energy of the inductor to load through diode D_o takes place.

$$I_L(t) = I_{\max} - \left(\frac{V_o - V_S}{L_r} \right) t \dots\dots\dots (4.29)$$

$$I_{Lr}(t) = I_{Lr}(t_6) - \left(\frac{V_o}{L_r}\right)t \dots\dots\dots(4.30)$$

$$I_L(t_6) = 0 \dots\dots\dots(4.31)$$

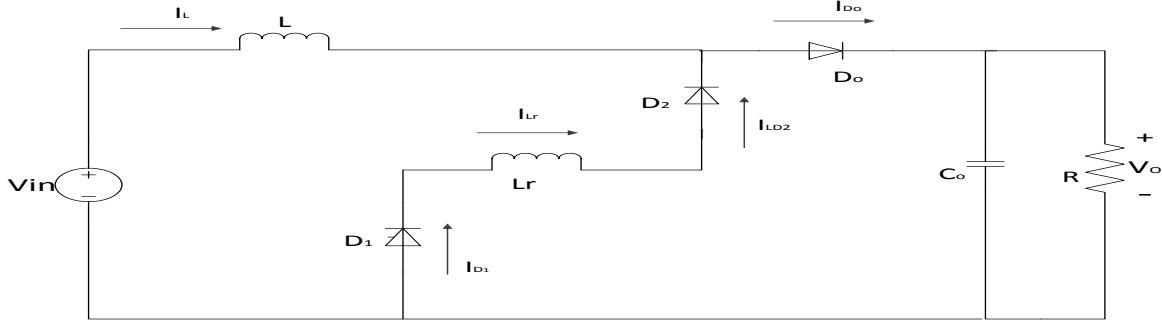


Fig. 4.7: Equivalent circuit of mode6 for interval [t₅-t₆]

4.4 Theoretical Waveforms

The Fig. 4.8 shows theoretical waveforms for one switching cycle. The theoretical curves for gate pulses, diode current, switch current and voltages, resonant inductor current and resonant capacitor voltage [4].

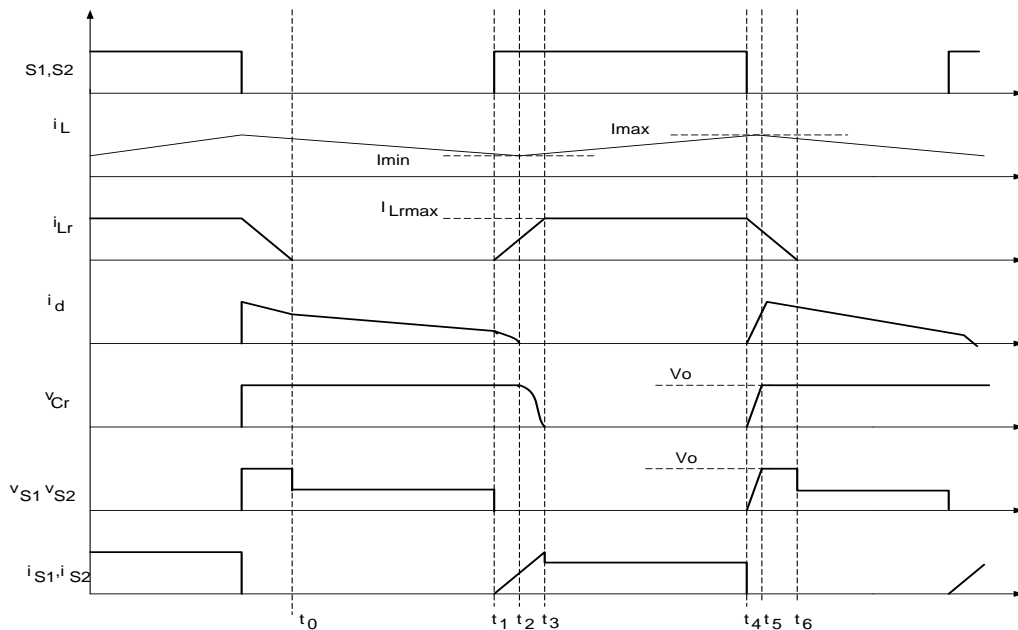


Fig. 4.8: Theoretical waveforms of converter

4.5 Converter Design

The specifications for the design of the converter are given in table 4.1. The specifications include converter output power rating, input voltage range, output voltage, allowable ripple percentage in current and voltage etc. Design of circuit includes two steps power circuit and auxiliary circuit respectively.

Table 4.1 Converter specifications for design

Sl. No.	Parameter	Specification	Value
1	Output power	P_{out}	60W
2	Output voltage	V_{out}	42V
3	Input voltage	V_{in}	15-25V
4	Switching frequency	F_{sw}	50kHz
5	Output voltage ripple	ΔV_o	5%
6	Input current peak ripple	ΔI_L	20%

4.5.1 Design of the Power Circuit

The power circuit consists of the main switch, boost diode, input inductor and the output capacitor. Here calculations for input inductor and output capacitor are shown.

Input inductor L:

The numerical value of the input inductor L must be decided first because its value sets the peak input current which the converter switches have to withstand and therefore this current is necessary to decide the rating of other power circuit components [3]. The maximum current without ripple is

$$I_{\max} = \frac{P_{out}}{V_{in}} = \frac{60}{15} = 4.34A \dots\dots\dots (4.32)$$

The maximum peak-peak ripple current is

$$\Delta I_{rpp} = \Delta I_L = I_{pk_max} \cdot \Delta I = 4.34 \times 20\% = 0.869A \dots\dots\dots (4.33)$$

Therefore the maximum peak input current with ripple is

$$I_{rpk_max} = I_{pk_max} + \frac{\Delta I_{rpp}}{2} = 4.34 + \frac{0.869}{2} = 4.774A \dots\dots\dots (4.34)$$

The duty ratio of the converter when the maximum current occurs is

$$D_{max} = 1 - \frac{V_{in_min}}{V_o} = 1 - \frac{15}{42} = 0.6428 \dots\dots\dots (4.35)$$

The input inductor value is calculated as follows

$$L = \frac{V_{in_min} \cdot D_{max}}{\Delta I_L \cdot f_{sw}} = \frac{15 \cdot 0.6428}{0.832 \cdot 50kHz} = 240\mu H \dots\dots\dots (4.36)$$

Output capacitor:

The output capacitor acts as an energy storage element. It stores energy when the input voltage and current are near their peak and provides this energy to the output load when the line is low. The point of reference for selection of capacitor is the endurable ripple in the output voltage. The peak charging current of the capacitor is

$$I_{chg_pk} = I_o = \frac{P_{out}}{V_{out}} = \frac{60}{42} = 1.428A \dots\dots\dots (4.37)$$

The output capacitor C₀ can be determined by

$$C < \frac{(1-D)V_o}{Rf_s \Delta V_o} \dots\dots\dots (4.38)$$

$$C < \frac{(1-D)I_o}{f_s \Delta V_o} \dots\dots\dots (4.39)$$

$$C < \frac{\left(1 - \frac{25}{42}\right) \times 1.428}{50 \times 10 \times (0.05 \times 42)} \dots\dots\dots (4.40)$$

$$C = 110 \mu F$$

4.5.2 Design of the auxiliary circuit

ZVS condition of switch:

Fig. 4.9 shows the ZVS condition in soft-switching converter. To satisfy ZVS condition, current through resonant inductor should be greater than main inductor current in interval 4. The following equations describe current and voltage of resonant inductor during this interval [1].

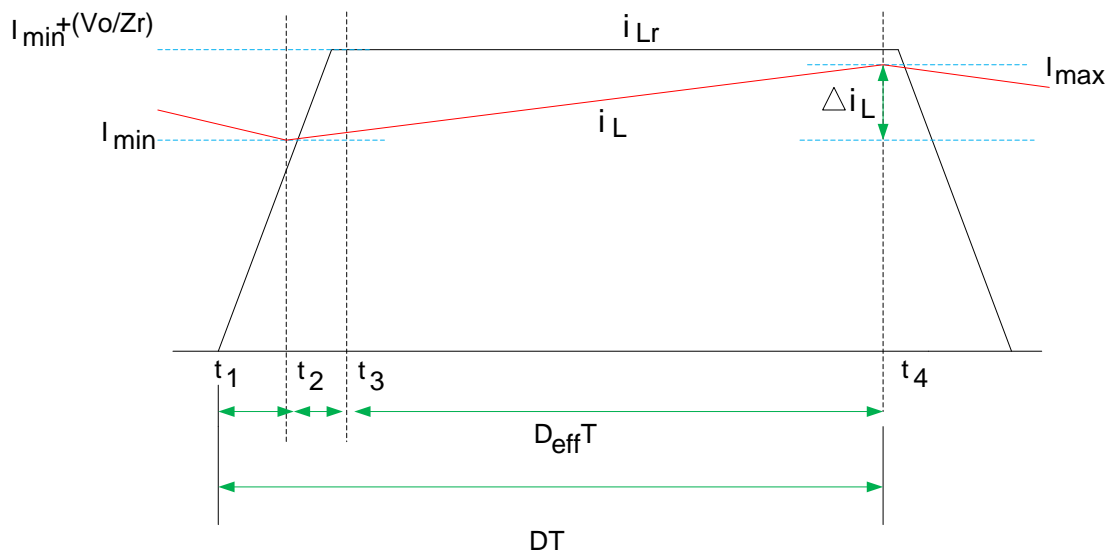


Fig. 4.9: ZVS condition of switch

$$D_{\min} = \left(\frac{V_o - V_{in,\max}}{V_o} \right) \dots\dots\dots (4.41)$$

$$D_{\min} = \left(\frac{42 - 25}{42} \right) = 0.404$$

$$D_{\max} = \left(\frac{V_o - V_{in,\min}}{V_o} \right) \dots\dots\dots (4.42)$$

$$D_{\max} = \left(\frac{42 - 15}{42} \right) = 0.6428$$

$$V_{Lr}(t) = V_{DS,sat} + V_F = V_{FW} \dots\dots\dots (4.43)$$

$$I_{Lr}(t) = -\frac{V_{FW}}{L_r} t + I_{\min} + \frac{V_o}{Z_r} > I_{\max} \dots\dots\dots (4.44)$$

$$I_{Lr}(t) = -\frac{V_{FW}}{L_r} D_{\max} T + I_{\min} + \frac{V_o}{Z_r} > I_{\max} \dots\dots\dots (4.45)$$

$$I_{\max} = I_{\min} + \Delta I_L - \frac{V_{FW}}{L_r} D_{\max} T + \frac{V_o}{Z_r} > \Delta I_L \dots\dots\dots (4.46)$$

Resonant inductor:

In Fig. 4.9, the time interval 2 is the rising time of resonant inductor current given by equation (4.47). To get maximum resonant current, the time interval 3, is selected as ¼ of the resonant period given by equation (4.48). For proper selection of resonant inductor, interval 2 and interval 3 collectively can be set to 10% of minimum on time period. Sometime it is selected as 50% of minimum on time [6].

$$t_3 - t_2 = \frac{L_r}{V_o} I_{\min} \dots\dots\dots (4.47)$$

$$t_4 - t_3 = \frac{T_r}{4} \dots\dots\dots (4.48)$$

$$\frac{L_r}{V_o} I_{\min} + \frac{T_r}{4} = 0.1 D_{\min} T \dots\dots\dots (4.49)$$

$$L_r < \frac{\frac{2}{\pi} D_{\min} T V_o - V_{FW} D_{\max} T}{\Delta I_L + \frac{2}{\pi} I_{\min}} \dots\dots\dots (4.50)$$

$$L_r < \frac{\left(\frac{2}{\pi} \times 0.404 \times \frac{1}{50 \times 10^3} \times 42\right) - \left(\frac{2.1 \times 0.6428}{50 \times 10^3}\right)}{0.832 + \left(\frac{2}{\pi} \times 2.52\right)} \dots\dots\dots (4.51)$$

$$L_r = 10 \mu H$$

Resonant capacitor:

The resonant capacitor is connected in parallel to the switch, so voltage of resonant capacitor and main switch will be similar at turn-off condition. To satisfy ZVS condition, it can be selected ten times of the output capacitance of the switch [1]. Simplified equation for resonant capacitor is given by equation (4.4)

$$C_r < \frac{0.04 D_{\min}^2 T^2 V_o}{\pi^2 L_r} + \frac{4 I_{\min}^2 L_r}{\pi^2 V_o^2} - \frac{0.8 I_{\min} D_{\min} T}{\pi^2 V_o} \dots\dots\dots (4.52)$$

$$C_r < \frac{0.04 \times (0.404)^2 \times \left(\frac{1}{50 \times 10}\right)^2 \times 42}{\pi^2 \times (10^{-5})} + \frac{4 \times 2.52^2 \times 10^{-5}}{\pi^2 \times 42^2} - \frac{0.8 \times 2.52 \times .404 \times \left(\frac{1}{50 \times 10^3}\right)}{\pi^2 \times 42}$$

$$C_r = 40 nF$$

4.6 Steady State Analysis of Converter

The output voltage of converter can be obtained by averaging voltage path of diode and inductor over a switching period [4]. The output voltage is assumed to a constant voltage source and can be derived as follows:

$$V_o = avg\{V_D\}_T - avg\{V_L\}_T + V_i \dots\dots\dots (4.53)$$

Where diode voltage average can be calculated as

$$avg\{V_D\}_T = \left\{ V_H \left[\sqrt{L_r C_r} \left(\frac{\pi}{2} - 1 \right) \right] + V_H (t_5 - t_3) + \left[-2I_L Z_r \sqrt{C_r} - V_H + 2I_L Z_r \sqrt{1 + \frac{V_H}{I_L Z_r}} \right] / \omega \right\} / T \dots\dots\dots (4.54)$$

Similarly inductor averaged voltage can be derived, above observation shows that design of output voltage is more difficult in case of soft switching techniques

$$D_{eff} = \frac{avg\{V_D\}_T}{V_H} \dots\dots\dots (4.55)$$

$$\Delta D = \left\{ -i_L L_r / V_H + \left[\arcsin \left(\frac{V_H}{V_H + 2I_L Z_r} \right) \right] / \omega + \left[\sqrt{4i_L^2 Z_r^2 + 4i_L Z_r V_H + 2I_L Z_r} \right] / V_H \omega \right\} / T \dots\dots\dots (4.56)$$

The output voltage of proposed converter in terms of D_{eff} is given by

$$V_o = \frac{1}{1 - D_{eff}} V_i \dots\dots\dots (4.57)$$

4.7 Specification of converter for Simulation

Table 4.1 includes specifications of converter which are used for simulating the circuit in Psim9.0.

Table 4.1 Converter specification for simulation

Sl. No.	Parameter	Specification	Value
1	Output power	P_{out}	60W
2	Output voltage	V_{out}	42V
3	Input voltage	V_{in}	15-25V
4	Switching frequency	F_{sw}	50kHz
5	Resonant inductor	L_r	10 μ H
6	Resonant capacitor	C_r	40nF
7	Main inductor	L	240 μ H
8	Output capacitor	C_0	110 μ F

4.8 Simulation Results

Output voltage of PV is given as input to converter circuit. Here simulation results of soft-switching converter are shown below. Fig. 4.10 shows the PWM signal given at gate terminal of switches S_1 and S_2 . Fig. 4.11 shows current waveforms of main inductor current.

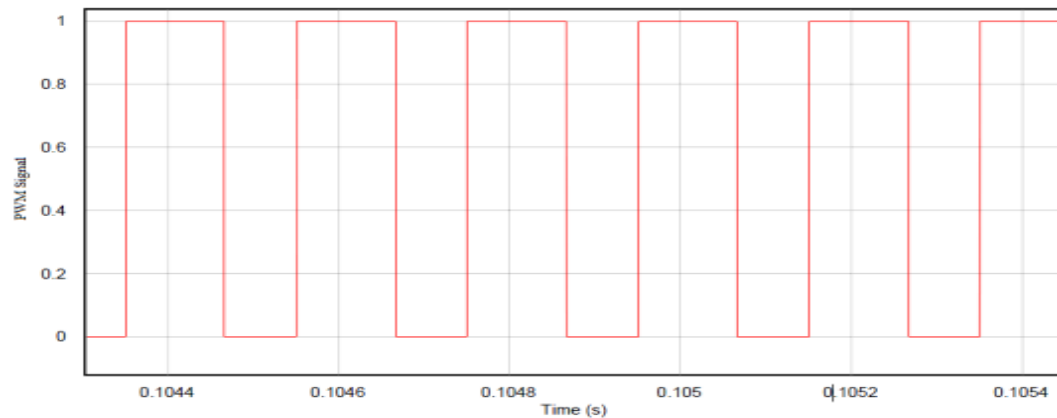


Fig. 4.10: PWM signal for switch S_1, S_2

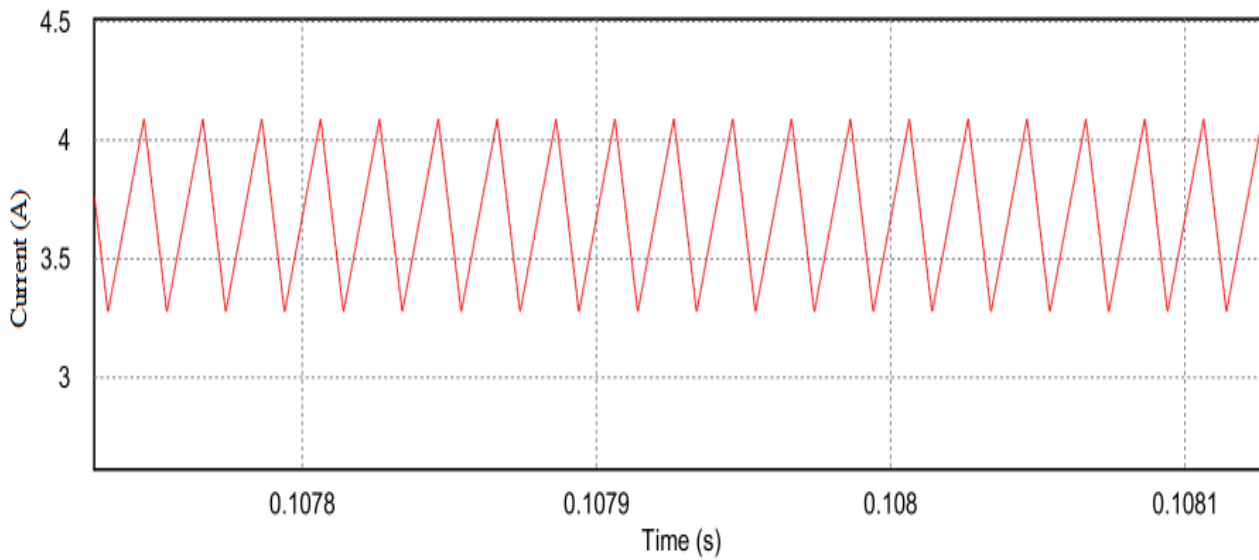


Fig. 4.11: Main inductor current

Fig. 4.12 shows voltage and current waveforms of switches S_1 and S_2 representing soft switching operation of switches.

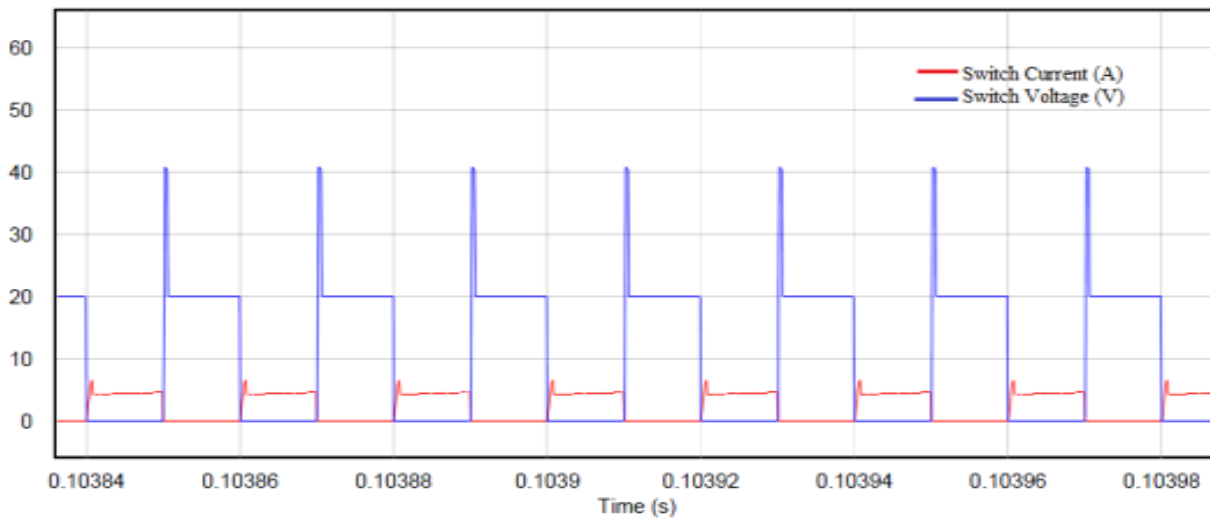


Fig. 4.12: Current and voltage across switch S_1, S_2

Fig. 4.13 shows switches S_1 and S_2 are turned on with ZCS. Here switch voltage changes 20V to zero whereas current is slowly rising due to linearly charged resonant inductor.

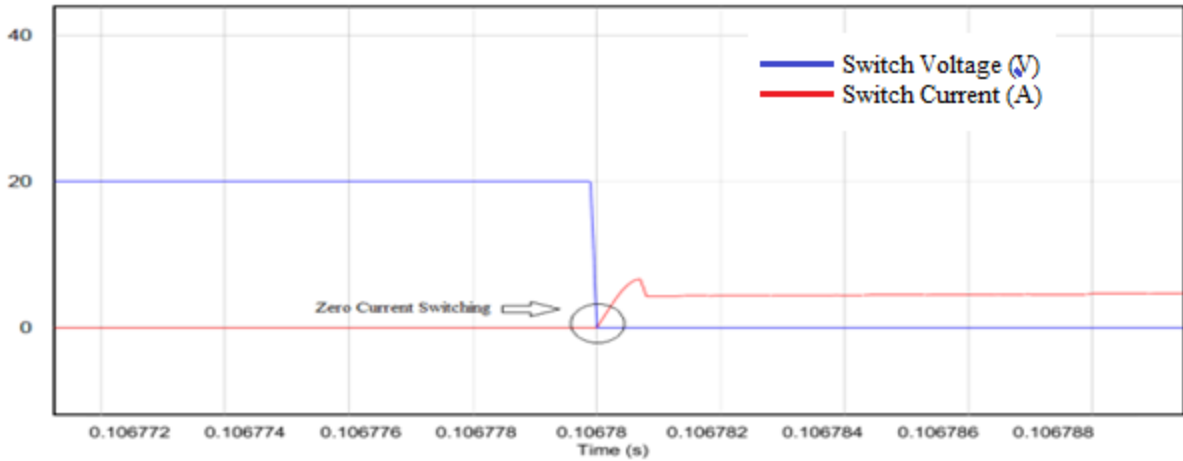


Fig. 4.13: ZCS for switches S_1, S_2 at turn on

Fig 4.14 shows switches S_1 and S_2 are turned on with ZCS. Here switch current changes 6A to zero whereas voltage is slowly rising due to linearly charged resonant capacitor.

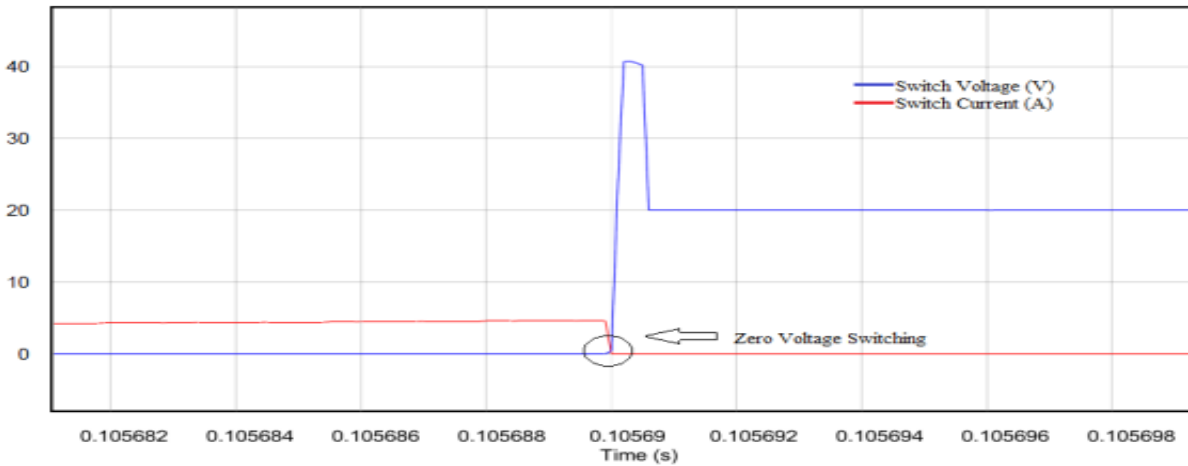


Fig. 4.14: ZVS operation for switches S_1, S_2 at turn off

Fig. 4.15 shows curve of resonant inductor current and resonant capacitor voltage, these elements make circuit to operate in resonance in mode 3 of operation. Fig. 4.16 shows the diode current and voltage waveforms simultaneously.

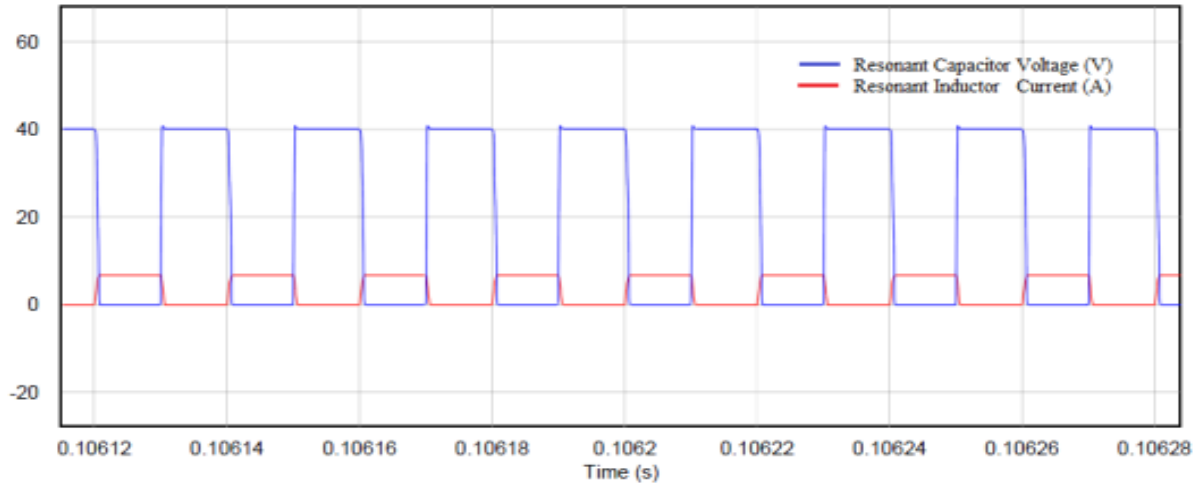


Fig. 4.15: Resonant inductor current and resonant capacitor voltage

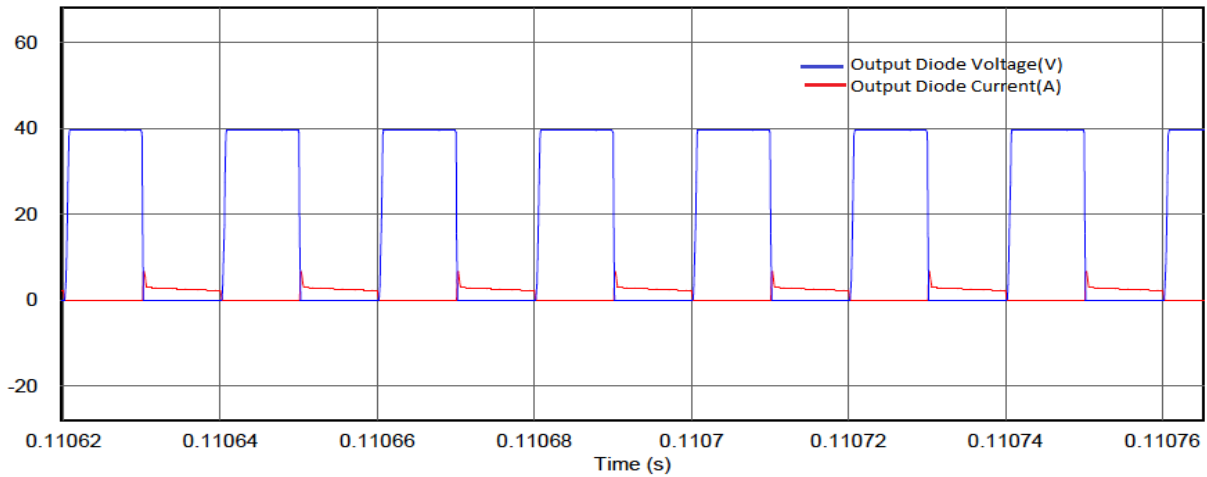


Fig. 4.16: Output diode voltage and current

Fig. 4.17 shows the output voltage waveform of soft switching converter which is obtained approximately 42 V when 21 V from PV given as input with duty ratio of 0.5 and 50 kHz of switching frequency. The efficiency of converter at full load is 95.9 %. Fig. 4.18 shows the output power of the converter at full load. The power at full load is 57.43 W.

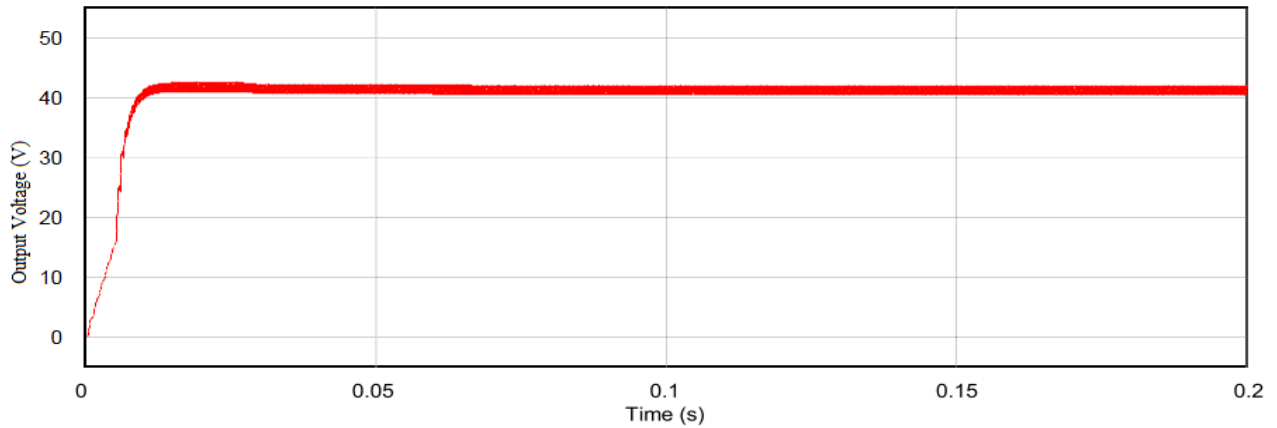


Fig. 4.17: Output voltage of converter

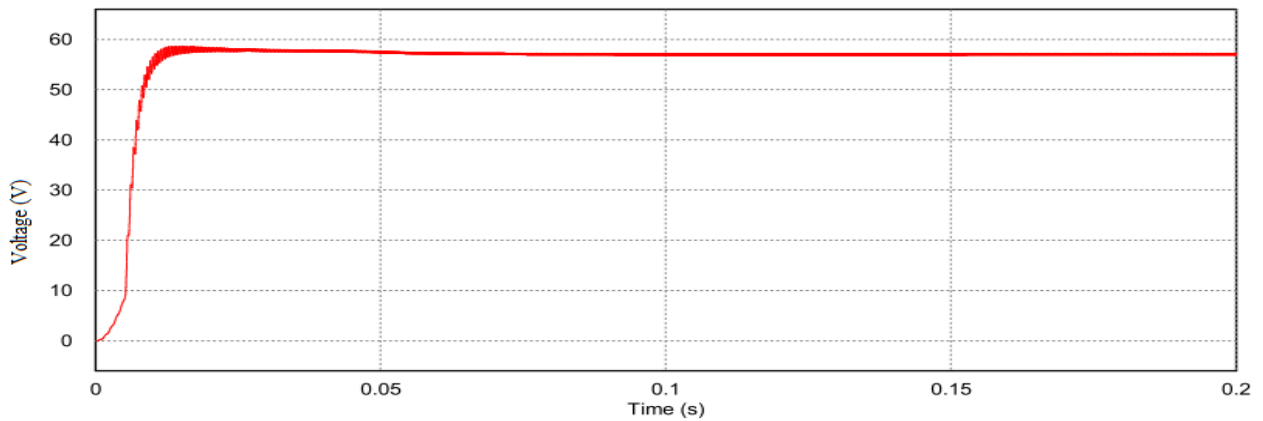


Fig. 4.18: Output power of converter

4.9 Tabulation for losses and efficiency in hard and soft switching

There are two types of losses which occur in soft-switching converter which are switching and conduction losses for calculation of these losses following formulas are used:

For calculation of switching losses in main and auxiliary switch

$$P_{sw} = V_0 \cdot I_0 \cdot F_{sw} \cdot \left(\frac{T_{on} + T_{off}}{2} \right)$$

For calculation of conduction losses in main and auxiliary switch

$$P_{sw_cond} = 1.8 \cdot I_{s_rms}^2 \cdot R_{on}$$

For calculation of conduction losses in diode

$$P_{D_cond} = V_F \cdot I_{D_avg}$$

Total losses can be determined after summing the calculated losses

$$P_{losses} = P_{sw} + P_{cond} + P_D$$

Later efficiency can be calculated using rated output power value and losses

$$\eta = \left(\frac{P_0}{P_0 + P_{losses}} \right) \times 100$$

Table 4.2 Comparison of hard and soft-switching

Sl. No.	Load (%)	Type of Switching	Power Losses P_{losses} (W)	Output Power P_o (W)	Efficiency $\eta(\%) = \left(\frac{P_0}{P_0 + P_{losses}} \right) \times 100$
1	20	Hard	1.33	12	90%
		Soft	0.806	12	93.7%
2	40	Hard	2.37	24	91%
		Soft	1.289	24	94.9%
3	60	Hard	3.29	36	91.61%
		Soft	1.735	36	95.4%
4	80	Hard	4.327	48	91.73%
		Soft	2.156	48	95.7%
5	100	Hard	5.359	60	91.8%
		Soft	2.565	60	95.9%

4.10 Tabulation for current and voltages stresses

The switching stresses in various element is calculated and tabulated in

Table 4.3 Current and voltage stresses of various elements

Sl. No.	Specification	Calculated Values
1	I_{base}	$I_{max} = 4.34A$
2	V_{base}	$V_o = 42V$
3	Voltage stresses of S_1, S_2, D_1, D_2 and D_o	$1.0(p.u)$
4	Current stresses of $S_1, S_2, D_1,$ and D_2	$1.0 + \frac{V_o \sqrt{\frac{C_r}{L_r}}}{I_{max}} = 1.17(p.u)$
5	Current stress of D_o	$2.0 + \frac{V_o \sqrt{\frac{C_r}{L_r}}}{I_{max}} = 2.17(p.u)$

4.11 Conclusion

In chapter soft switching boost converter is discussed. Operation modes with block diagram of the proposed system are illustrated. Theoretical waveform presenting the operational intervals is described. Simulation results of circuit with PV and MPPT is presented. Efficiency calculation is done for converter circuit and tabulated, which shows higher efficiency for soft switching converter.

CHAPTER-5

CONCLUSION

5.1 Conclusion

In this project simulation and design of soft switching converter is done. Efficiency of hard switching and soft switching converters are compared at varying load conditions, in which efficiency for designed soft switching converter is found to be much higher. Switching curves for converter circuit. Switching curves for soft-switching circuit are gradual which decreases di/dt and dv/dt rating and hence reduction in EMI achieved.

5.2 Scope for Future Work

In further work, proposed converter can be used as interleaved boost converter by connecting two such converters in parallel, this connection may result more increase in efficiency. A PID controller can be designed for the converter circuit for more stabilized output and its robustness can be verified. To get isolation without using transformers, coupled inductor topology can be constructed using designed circuit. The designed circuit can be used in stand-alone and grid connected PV system. The circuit can be used for power factor correction by slight modification.

REFERENCES

- [1] S.H. Park, G.R. Cha, Y.C. Jung and C.Y. Won, "Design and Application from PV Generation System Using a Soft-Switching Boost Converter with SARC", *IEEE Transactions on Industrial Electronics*, vol.57, no.2, pp. 515-522, Feb. 2010.
- [2] P.K. Jain; G. Joos, "A zero voltage transition boost converter employing a soft switching auxiliary circuit with reduced conduction losses," *IEEE Transactions on Power Electronics*, vol.19, no.1, pp.130-139, Jan. 2004.
- [3] A. Tomaszu, K. Maszuka, "High efficiency high step-up DC/DC converters – a review," *Bulletin Of Polish Academy Of Sciences*, Vol. 59, no. 4, pp. 475-483, Feb. 2011.
- [4] Y. M. Chang, J.Y. Lee, W.L. Tsai and Y. Y. Sun, "Design and analysis of H-soft-switched converters" *IEEE Proceeding Electronics Power Appliances*, vol. 142, no. 4, pp. 255-262, Jul. 1995.
- [5] Y.C. Jung, J.G. Cho, G. H. Cho, "Zero voltage switching resonant dc-link inverter with low voltage", *Industrial Electronics Control and Instrumentation 1991 proceeding IECON*, vol.1, no. 2, pp.308-313, 1991.
- [6] J.S. Yu, S.R. Park, Y.C. Jung and C.Y. Won, S.H. Park, "Analysis and design of a soft switching boost converter with an HI-bridge auxiliary resonant circuit," *IEEE Transaction on Power Electronics*, vol. 25, no. 8, pp. 2142-2149, Aug. 2010.
- [7] H. Bodur and A. FarukBakan, "A new ZCT-ZVT-PWM DC–DC converter", *IEEE Transaction on Power Electronics*, vol. 19, no. 3, pp. 676–684, May 2004.
- [8] B. R. Lin and J. J. Chen, "Analysis and implementation of a soft switching converter with high-voltage conversion ratio," *IET Power Electronics*, vol. 1, no. 3, pp. 386–394, Sep. 2008.
- [9] G.Moschopoulos, P.Jain, Y.Liu and Geza Joos, "A Zero Voltage Switched PWM Boost Converter with an Energy Feedforward Auxiliary Circuit," *IEEE Transactions on Power Electronics*, vol.14, pp. 653-662, Jul. 1999.
- [10] M. Veerachary, "Design of Robust Digital PID Controller for H-Bridge Soft-Switching Boost Converter, *Transactions on Industrial Electronics* , vol. 58, No. 7, July 2010.
- [11] E. Adib and H. Farzanehfard, "Family of zero-current transition PWM converters," *IEEE Transaction On Industrial Electronics*, vol. 55, no. 8, pp. 3055–3063, Aug. 2008.

- [12] R. D. Middlebrook, "Transformerless dc-to-dc converters with large conversion ratios," *IEEE Transaction on Power Electronics*, vol. 3, no. 4, pp. 484–488, Oct. 1988.
- [13] M. D. Bellar, T.S. Wu, A. Tchamdjou, J. Mahdavi, and M. Ehsani, "A review of soft-switched DC-AC converters", *IEEE Transaction On Industry Applications*, vol. 34, no. 4, pp. 847–960, Aug. 1998.
- [14] M. G. Villalva, J. R. Gazoli and E. R. Filho, "Comprehensive Approach to Modeling and Simulation of PV Arrays", *IEEE Transactions on Power Electronics*, vol.24, no.5, pp. 1036-1043, May 2009.
- [15] Salam Z., Ishaque K. and Taheri H., "An improved two-diode photovoltaic (PV) model for PV system," *Power Electronics, Drives and Energy Systems (PEDES) & 2010 Power India, 2010 Joint International Conference*, vol.3, no.4, pp.1,5, 20-23 Dec. 2010.
- [16] S. Sheik Mohammed, "Modeling and Simulation of Photovoltaic module using MATLAB/Simulink," *International Journal of Chemical and Environmental Engineering*, Vol.2, no.5, pp.486-494, Oct. 2011.
- [17] T. Esum and P. L. Chapman, "Comparison of photovoltaic array maximum power point tracking techniques," *IEEE Transaction on Energy Conversion*, vol. 22, no. 2, pp. 2036-2044, Jun. 2007.
- [18] S. S. D, "Modeling and Simulation of Incremental Conductance MPPT Algorithm for Photovoltaic Applications", *International Journal of Scientific Engineering and Technology*, Vol.2, no.7, pp. 681-685, Jul. 2013.
- [19] J. Surya Kumari, Dr. Ch. Sai Babu, A. Kamalakarbabu, "Design and analysis of P&O and IP&O MPPT techniques for PV system", *International Journal of Modern Engineering research*, vol.2, no. 4, pp. 2174-2180, Aug. 2012.
- [20] W. Xiao, N. Ozog, and W. G. Dunford, "Topology study of photovoltaic interface for maximum power point tracking," *IEEE Transaction on Industrial Electronics*, vol. 54, no. 3, pp. 1696-1704, Jun. 2007.
- [21] A Safari and S. Mekhilef, "Simulation and hardware implementation of incremental conductance MPPT with direct control method using cuk converter," *IEEE Transaction on Industrial Electronics*, vol. 58, no. 4, pp. 286-295, Apr. 2011.
- [22] A. Rodriguez and G. A. J. Amaratunga, "Analytic solution to the photovoltaic maximum power point problem," *IEEE Transaction on Circuits and Systems-I*, vol. 54, no. 9, pp. 2054-2060, Sep. 2007.